

# VIBRATIONS OF CRACKED FUNCTIONALLY GRADED BEAMS: GENERAL SOLUTION AND APPLICATION – A REVIEW

Nguyen Tien Khiem<sup>1,\*</sup> 

<sup>1</sup>*Vietnam Association for Mechanics (VAM), 264 Doi Can, Ba Dinh, Hanoi, Vietnam*

\*E-mail: [ntkhiem@imech.vast.vn](mailto:ntkhiem@imech.vast.vn)

Received: 28 December 2022 / Published online: 30 December 2022

**Abstract.** This paper presents a unified approach to vibration analysis of functionally graded beams with transverse open-edge cracks based on the so-called vibration shape obtained as a general solution of vibration equations in the frequency domain. The crack is modeled by a pair of translational and rotational springs of stiffness computed from the crack depth in dependence upon functionally graded material parameters. The frequency-dependent vibration shape functions allow one not only to obtain the closed-form solution of both free and forced vibrations for multiple cracked FGM beams but also to develop the well-known methods such as Transfer Matrix Method or Dynamic Stiffness Method for analysis of FGM framed structures. The proposed theoretical developments have been illustrated by their application for modal analysis and frequency response analysis of multi-span and multistep beams.

*Keywords:* functionally graded materials, vibration shape functions, modal analysis, frequency response, multiple cracked beams.

## 1. INTRODUCTION

The crack, which usually appears in many structural components, is a kind of damage that may lead a structure to collapse if it is not early detected. Nevertheless, the conventional (local) nondestructive techniques are difficult to apply for detecting cracks in huge or complicated structures [1–3]. Therefore, a more global approach such as the dynamic testing technique integrated with the system identification method is needed for the crack detection problem [4]. Obviously, when the integrated approach has been engaged, a model of a structure with cracks and dynamics of the cracked structure becomes essential [5, 6]. At the early stage, a crack was treated purely as a change in the geometry of a structure [7], but then, researchers recognized that crack may also change the stress and strain distributions in the vicinity of the cracked section. Based on this idea, Christides and Barr proposed the so-called one-dimensional theory of cracked beam [8] and then, Shen and Pierrie used the theory for free vibration analysis of cracked

beam [9,10]. On the other hand, numerous investigators, for example, Irwin [11], Westmann and Yang [12], Dimarogonas and Paipetis [13], etc, revealed that a crack on a beam element significantly increases the flexibility due to the strain energy concentration at the crack tip under load. This concept of crack allows not only straightforward analysis of cracked structures by the finite element method [14] but also developing various useful models of a crack in beam elements. Namely, an equivalent spring model of a concentrated crack was adopted in [15–18] where stiffness of the springs is calculated from the strain energy released by the crack. Another model of local crack on beam, that was treated as a singularity of beam stiffness, has been adopted in [19,20] and used for obtaining closed form solution of vibration modes for cracked beams. The spring model of concentrated crack was successfully employed for solving numerous problems of vibration in cracked Euler-Bernoulli [21–26] and Timoshenko [27–31] beams. The closed-form solutions for the vibration mode of multiple cracked homogeneous beams have been obtained in [26,31] respectively for Euler–Bernoulli and Timoshenko beams.

The present paper addresses establishing the closed-form solution of vibration mode for cracked beams made of functionally graded material (FGM) and applying it for solving both free and forced vibration of the structures. Though many problems related to cracked functionally graded beams have been solved [32–44], the equivalent spring model of crack has been adequately constructed in dependence upon the material parameters only in Ref. [45]. The established model of crack in FGM has been employed for vibration analysis of cracked functionally graded beams [46–48] and the beams with piezoelectric layer [49,50]. Moreover, the obtained general solution for vibration mode of cracked FGM beam allows one to develop the well-known transfer matrix method and dynamic stiffness method for vibration analysis of cracked FGM beam-like structures.

## 2. GENERAL SOLUTION FOR VIBRATION SHAPE

The vibration shape of an elastic structure is acknowledged as solution of free vibration problem in the frequency domain and, therefore, it is frequency-dependent function of spatial coordinates in the structure domain. Applying boundary conditions for the vibration shape we obtain the so-called frequency equation, solution of which gives rise to the natural frequencies of the structure under consideration. Substituting a specific natural frequency to the vibration shape yields the mode shape corresponding to the natural frequency. Moreover, the vibration shapes are employed as frequency-dependent shape functions for constructing the dynamic stiffness model of a structure that was proved to be more exact than the well-known finite element model.

Thus, in the present section general vibration shape is conducted for cracked beams of different types such as Euler-Bernoulli, Timoshenko, FGM and piezoelectric beams. Cracks in all the above-mentioned beam-type structures are transversally edged and modeled by equivalent springs of stiffness calculated from the crack depth in accordance with the theory of fracture mechanics. The most advantage of the crack model is that cracks are accounted-for in the form of conditions constraining the vibration shapes at the cracked cross-section.

## 2.1. Homogeneous beams

### 2.1.1. Euler-Bernoulli beams

It is well-known that the free bending vibration of Euler-Bernoulli beam in the frequency domain is described by the equation

$$\phi^{(IV)}(x) - \lambda^4 \phi(x) = 0, \quad x \in (0,1), \quad \lambda = L^4 \sqrt{\rho F \omega^2 / EI}, \quad (1)$$

for determining vibration shape  $\phi(x, \omega)$ .

Assume, furthermore, that the beam has been cracked at sections  $e_j, j = 1, 2, 3, \dots, n$  and cracks are represented by rotational springs of stiffness  $K_j$ . So that, solution of Eq. (1) must satisfy conditions

$$\begin{aligned} \phi(e_j + 0, \omega) &= \phi(e_j - 0, \omega), \\ \phi''(e_j + 0, \omega) &= \phi''(e_j - 0, \omega), \\ \phi'''(e_j + 0, \omega) &= \phi'''(e_j - 0, \omega), \\ \phi'(e_j + 0, \omega) &= \phi'(e_j - 0, \omega) + \gamma_j \phi''(e_j + 0, \omega), \end{aligned} \quad (2)$$

where so-called crack magnitude  $\gamma_j$  are calculated as

$$\begin{aligned} \gamma_j &= EI / LK_j = 6\pi (1 - \nu_0^2) (h/L) f_b(a_j/h), \\ f_b(z) &= z^2 \left( 0.6272 - 1.04533z + 4.5948z^2 - 9.9736z^3 + 20.2948z^4 \right. \\ &\quad \left. - 33.0351z^5 + 47.1063z^6 - 40.7556z^7 + 19.6z^8 \right). \end{aligned}$$

Letting  $\phi_0(x, \omega)$  denote solution of Eq. (1) for uncracked beam and introducing the function

$$K(x) = 0 \text{ for } x < 0 \text{ and } = S(x) \text{ for } x \geq 0 \text{ with } S(x) = (1/2\lambda) (\sinh \lambda x + \sin \lambda x), \quad (3)$$

one can prove that solution of Eq. (1) is represented in the form

$$\phi(x, \omega) = \phi_0(x, \omega) + \sum_{j=1}^n \mu_j K(x - e_j), \quad (4)$$

where so-called damage parameters  $\mu_j, j = 1, 2, 3, \dots, n$  are determined by the recurrent formula

$$\mu_j = \gamma_j \left[ \phi''_0(e_j, \omega) + \sum_{k=1}^{j-1} \mu_k S''(e_j - e_k) \right], \quad j = 1, \dots, n. \quad (5)$$

On the other hand, it was well-known that general solution of Eq. (1) for uncracked beam is expressed as

$$\phi_0(x, \omega) = C_1 \cosh \lambda x + C_2 \sinh \lambda x + C_3 \cos \lambda x + C_4 \sin \lambda x,$$

with constants  $C_1, C_2, C_3, C_4$  determined by boundary conditions. So, if the damage parameters  $\mu_j$  is represented in the form  $\mu_j = C_1 \mu_{j1} + C_2 \mu_{j2} + C_3 \mu_{j3} + C_4 \mu_{j4}, j = 1, 2, \dots, n$ ,

then parameters  $\mu_{jk}, k = 1, 2, 3, 4$  are calculated as

$$\begin{aligned} \mu_{j1} &= \gamma_j \left[ \lambda^2 \cosh \lambda e_j + \sum_{k=1}^{j-1} \mu_{k1} S''(e_j - e_k) \right], \quad \mu_{j2} = \gamma_j \left[ \lambda^2 \sinh \lambda e_j + \sum_{k=1}^{j-1} \mu_{k2} S''(e_j - e_k) \right], \\ \mu_{j3} &= \gamma_j \left[ -\lambda^2 \cos \lambda e_j + \sum_{k=1}^{j-1} \mu_{k3} S''(e_j - e_k) \right], \quad \mu_{j4} = \gamma_j \left[ -\lambda^2 \sin \lambda e_j + \sum_{k=1}^{j-1} 4S''(e_j - e_k) \right], \end{aligned} \tag{6}$$

and solution (4) can be rewritten as

$$\phi(x, \omega) = C_1 \Phi_1(\lambda x) + C_2 \Phi_2(\lambda x) + C_3 \Phi_3(\lambda x) + C_4 \Phi_3(\lambda x), \tag{7}$$

where  $\Phi_k(\lambda x), k = 1, 2, 3, 4$  are

$$\begin{aligned} \Phi_1(\lambda x) &= \cosh \lambda x + \sum_{j=1}^n \mu_{j1} K(x - e_j), \quad \Phi_2(\lambda x) = \sinh \lambda x + \sum_{j=1}^n \mu_{j2} K(x - e_j), \\ \Phi_3(\lambda x) &= \cos \lambda x + \sum_{j=1}^n \mu_{j3} K(x - e_j), \quad \Phi_4(\lambda x) = \sin \lambda x + \sum_{j=1}^n \mu_{j4} K(x - e_j). \end{aligned} \tag{8}$$

So, an explicit expression of general vibration shape of multiple cracked Euler-Bernuolli beam has been obtained in the form of Eq. (7) with functions  $\Phi_k(\lambda x), k = 1, 2, 3, 4$  determined by Eq. (8) and damage parameters  $\mu_{jk}, j = 1, 2, 3, \dots, n; k = 1, 2, 3, 4$  calculated by formulas (6).

Moreover, four equations in (6) can be rewritten in the matrix form

$$[\mathbf{B}] \{\boldsymbol{\mu}_k\} = \{\mathbf{b}_k\}, \quad k = 1, 2, 3, 4, \tag{9}$$

where  $\boldsymbol{\mu}_k = \{\mu_{1k}, \dots, \mu_{nk}\}^T, \mathbf{B} = [b_{ij}, i, j = 1, 2, 3, \dots, n]$  is  $n \times n$ -matrix with elements

$$b_{ij} = \{1 \text{ if } i = j; 0 \text{ for } i < j; -\gamma_i S''(e_i - e_j) \text{ for } i > j\}, \tag{10}$$

and vectors  $\mathbf{b}_k, k = 1, 2, 3, 4$  are

$$\begin{aligned} \{\mathbf{b}_1\} &= \lambda^2 \{\gamma_1 \cosh \lambda e_1, \dots, \gamma_n \cosh \lambda e_n\}^T, \quad \{\mathbf{b}_2\} = \lambda^2 \{\gamma_1 \sinh \lambda e_1, \dots, \gamma_n \sinh \lambda e_n\}^T, \\ \{\mathbf{b}_3\} &= -\lambda^2 \{\gamma_1 \cos \lambda e_1, \dots, \gamma_n \cos \lambda e_n\}^T, \quad \{\mathbf{b}_4\} = -\lambda^2 \{\gamma_1 \sin \lambda e_1, \dots, \gamma_n \sin \lambda e_n\}^T. \end{aligned} \tag{11}$$

So, in case if crack parameters such as positions and magnitudes are given the damage parameters  $\mu_{jk}$  are evaluated by solving equation (9)–(11).

### 2.1.2. Timoshenko beams

For Timoshenko beam, the frequency domain equations of motion are

$$\omega^2 \rho W(x) + \kappa G (W'' - \Theta') = 0, \quad \omega^2 \rho I \Theta(x) + EI \Theta''(x) + \kappa GA (W' - \Theta) = 0, \tag{12}$$

and conditions at crack positions get the form

$$\begin{aligned} W(e_j + 0) &= W(e_j - 0) = W(e_j), \quad \Theta'_x(e_j + 0) = \Theta'_x(e_j - 0) = \Theta'(e_j), \\ \Theta(e_j + 0) &= \Theta(e_j - 0) + \gamma_j \Theta'_x(e_j), \quad W'_x(e_j + 0) = W'_x(e_j - 0) + \gamma_j \Theta'_x(e_j), \quad \gamma_j = EI/K_j. \end{aligned} \tag{13}$$

In this general solution of Eq. (12) for uncracked beam can be found in the form

$$\begin{aligned} W_0(x) &= C_1 \cosh k_1 x + C_2 \sinh k_1 x + C_3 \cos k_2 x + C_4 \sin k_2 x, \\ \Theta_0(x) &= r_1 C_1 \sinh k_1 x + r_1 C_2 \cosh k_1 x + r_2 C_3 \sin k_2 x - r_2 C_4 \cos k_2 x, \end{aligned} \quad (14)$$

$$\begin{aligned} r_1 &= (\rho\omega^2 / \kappa G k_1 + k_1), \quad r_2 = (\rho\omega^2 / \kappa G k_2 - k_2), \\ k_1 &= \sqrt{(\sqrt{b^2 + 4c} - b) / 2}, \quad k_2 = \sqrt{(\sqrt{b^2 + 4c} + b) / 2}, \\ b &= \alpha(1 + \beta), \quad c = \alpha(\tau - \alpha\beta), \quad \alpha = \rho\omega^2 / E, \quad \beta = E / \kappa G, \quad \tau = A / I. \end{aligned} \quad (15)$$

Using the notations

$$\begin{aligned} S_w(x) &= S_1 \sinh k_1 x + S_2 \sin k_2 x, \quad S_\theta(x) = r_1 S_1 \cosh k_1 x - r_2 S_2 \cos k_2 x, \\ S_1 &= (r_2 + k_2) / (r_1 k_2 + r_2 k_1), \quad S_2 = (r_1 - k_1) / (r_1 k_2 + r_2 k_1), \end{aligned} \quad (16)$$

it can be proved that general solution of Eq. (12) satisfying conditions (13) is

$$W(x, \omega) = C_1 W_1(k_1, x) + C_2 W_2(k_1, x) + C_3 W_3(k_2, x) + C_4 W_4(k_2, x), \quad (17)$$

$$\Theta(x, \omega) = C_1 \Theta_1(k_1, x) + C_2 \Theta_2(k_1, x) + C_3 \Theta_3(k_2, x) + C_4 \Theta_4(k_2, x), \quad (18)$$

where

$$W_1(x) = \cosh k_1 x + \sum_{j=1}^n \mu_{1j} K_w(x - e_j), \quad W_2(x) = \sinh k_1 x + \sum_{j=1}^n \mu_{2j} K_w(x - e_j), \quad (19)$$

$$W_3(x) = \cos k_2 x + \sum_{j=1}^n \mu_{3j} K_w(x - e_j), \quad W_4(x) = \sin k_2 x + \sum_{j=1}^n \mu_{4j} K_w(x - e_j),$$

$$\Theta_1(x) = r_1 \sinh k_1 x + \sum_{j=1}^n \mu_{1j} K_\theta(x - e_j), \quad \Theta_3(x) = r_2 \sin k_2 x + \sum_{j=1}^n \mu_{3j} K_\theta(x - e_j), \quad (20)$$

$$\Theta_2(x) = r_1 \cosh k_1 x + \sum_{j=1}^n \mu_{2j} K_\theta(x - e_j), \quad \Theta_4(x) = -r_2 \cos k_2 x + \sum_{j=1}^n \mu_{4j} K_\theta(x - e_j),$$

$$K_w(x) = \{0: x < 0; S_w(x) : x \geq 0\}, \quad K'_w(x) = \{0: x < 0; S'_w(x) : x \geq 0\},$$

$$K_\theta(x) = \{0: x < 0; S_\theta(x) : x \geq 0\}, \quad K'_\theta(x) = \{0: x < 0; S'_\theta(x) : x \geq 0\},$$

$$\mu_{kj} = \gamma_j \left\{ L_k(e_j) + \sum_{i=1}^{j-1} \mu_{ki} S'_\theta(e_j - e_i) \right\}; \quad k = 1, 2, 3, 4; j = 1, 2, \dots, n.$$

$$L_1(x) = k_1 r_1 \cosh k_1 x, \quad L_2(x) = k_1 r_1 \sinh k_1 x, \quad L_3(x) = k_2 r_2 \cos k_2 x, \quad L_4(x) = k_2 r_2 \sin k_2 x. \quad (21)$$

## 2.2. Functionally graded Timoshenko beams

### 2.2.1. Governing equations

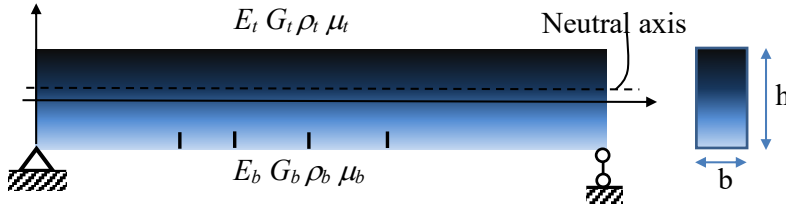


Fig. 1. Multiple cracked FGM beam model

Let's consider a Timoshenko beam made of functionally graded material as shown in Fig. 1 with mechanical properties varying accordingly to the power law along the beam thickness

$$\mathfrak{I}(z) = \mathfrak{I}_b + (\mathfrak{I}_t - \mathfrak{I}_b)V(z), \quad V(z) = (z/h + 1/2)^n, \quad -h/2 \leq z \leq h/2, \quad (22)$$

where  $\mathfrak{I}$  stands for elasticity ( $E$ ), shear ( $G$ ) modulus and material density ( $\rho$ ) and indexes  $t$  and  $b$  denote the top and bottom materials;  $z$  is ordinate of the point from the central axis and  $h$  is the beam thickness.

Accordingly, the Timoshenko beam theory represented by the relationships

$$u(x, z, t) = u_0(x, t) - (z - h_0)\theta(x, t), \quad w(x, z, t) = w_0(x, t), \quad (23)$$

with  $u_0(x, t)$ ,  $w_0(x, t)$  being the displacements on neutral axis located at the high  $h_0$  from the central axis;  $\theta$  is slope of the cross-section, allows the constituting equations be established in the form

$$\begin{aligned} \varepsilon_x &= \partial u_0 / \partial x - (z - h_0) \partial \theta / \partial x, & \gamma_{xz} &= \partial w_0 / \partial x - \theta, \\ \sigma_x &= E(z) \varepsilon_x, & \tau_{xz} &= \psi G(z) \gamma_{xz}. \end{aligned} \quad (24)$$

Using Hamilton principle, equations for free vibration of a uniform beam segment can be established in the form

$$I_{11} \ddot{u} - A_{11} u'' - I_{12} \ddot{\theta} = 0, \quad I_{12} \ddot{u} - I_{22} \ddot{\theta} + A_{22} \theta'' + A_{33} (w' - \theta) = 0, \quad I_{11} \ddot{w} - A_{33} (w'' - \theta') = 0, \quad (25)$$

where

$$\begin{aligned} A_{11} &= bhE_b (R_E + n) / (1 + n), \quad A_{33} = bh\psi G_b (R_G + n) / (1 + n), \quad R_E = E_t / E_b, \quad R_G = G_t / G_b, \\ A_{22} &= bh^3 E_b [(3R_E + n) / 3(3 + n) - (2R_E + n) / (2 + n) \alpha + (R_E + n) / (1 + n) \alpha^2], \\ \alpha &= 1/2 + h_0/h, \quad I_{11} = bh\rho_b (R_\rho + n) / (1 + n), \\ I_{12} &= bh^2 \rho_b [(2R_\rho + n) / 2(2 + n) - (R_\rho + n) / (1 + n) \alpha], \quad R_\rho = \rho_t / \rho_b, \\ I_{22} &= bh^3 \rho_b [(3R_\rho + n) / 3(3 + n) - (2R_2 + n) / (2 + n) \alpha + (R_2 + n) / (1 + n) \alpha^2], \\ h_0 &= [n(R_E - 1) / 2(n + 2)(n + R_E)]h. \end{aligned} \quad (26)$$

Seeking solution of (25) in the form  $u(x, t) = U(x, \omega)e^{i\omega t}$ ,  $w(x, t) = W(x, \omega)e^{i\omega t}$ ,  $\theta(x, t) = \Theta(x, \omega)e^{i\omega t}$  one gets

$$(\omega^2 I_{11}U + A_{11}U'') - \omega^2 I_{12}\Theta = 0, \quad (\omega^2 I_{22}\Theta + A_{22}\Theta'') - \omega^2 I_{12}U + A_{33}(W' - \Theta) = 0, \\ \omega^2 I_{11}W + A_{33}(W'' - \Theta') = 0,$$

or

$$[\mathbf{A}_2] \{ \mathbf{Z}'' \} + [\mathbf{A}_1] \{ \mathbf{Z}' \} + [\mathbf{A}_0] \{ \mathbf{Z} \} = 0, \tag{27}$$

with  $\{ \mathbf{Z}(x, \omega) \} = \{ U(x, \omega), \Theta(x, \omega), W(x, \omega) \}^T$  and

$$[\mathbf{A}_2] = \begin{bmatrix} A_{11} & 0 & 0 \\ 0 & -A_{22} & 0 \\ 0 & 0 & A_{33} \end{bmatrix}, \quad [\mathbf{A}_1] = \begin{bmatrix} 0 & 0 & 0 \\ 0 & 0 & -A_{33} \\ 0 & -A_{33} & 0 \end{bmatrix}, \\ [\mathbf{A}_0] = \begin{bmatrix} \omega^2 I_{11} & -\omega^2 I_{12} & 0 \\ \omega^2 I_{12} & A_{33} - \omega^2 I_{22} & 0 \\ 0 & 0 & \omega^2 I_{11} \end{bmatrix}.$$

Obviously, due to functionally graded properties of the beam material the axial (longitudinal) and flexural (bending) vibration modes in FGM beams are coupled and their coupling is characterized by the coefficient  $I_{12}$  that equals to zero if  $E_t = E_b$  or  $n = 0$  corresponding to the case of homogeneous beams. Additionally, the neutral plane position in FGM beams has deviated from the central one at a distance calculated by expression (26) that also becomes zero for homogeneous beams.

**2.2.2. Crack model in functionally graded beams**

Assume furthermore that the functionally graded beam is damaged to edge-open cracks of depth  $a_1, \dots, a_n$  at positions  $e_1, \dots, e_n$ . Because of coupling of axial and transverse vibrations in the functionally graded beam, see Eq. (25), crack at position  $e_j$  should be represented by a pair of equivalent springs, one is a translational spring of stiffness  $T_j$  and other is a rotational one of stiffness  $R_j$  (Fig. 2).

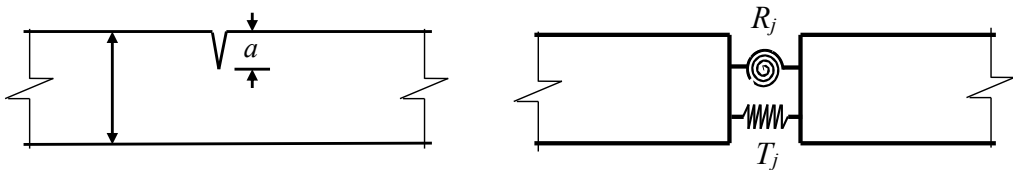


Fig. 2. Model of open edge crack in functionally graded beam

Thus, conditions should be satisfied at the crack position are [46]

$$U(e_j + 0) = U(e_j - 0) + \gamma_{aj}U'_x(e_j), \quad \Theta(e_j + 0) = \Theta(e_j - 0) + \gamma_{bj}\Theta'_x(e_j), \\ \Theta'_x(e_j + 0) = \Theta'_x(e_j - 0), \quad W'_x(e_j + 0) = W'_x(e_j - 0) + \gamma_{bj}\Theta'_x(e_j). \tag{28}$$

where  $\gamma_{aj} = A_{11}/T_j$ ,  $\gamma_{2j} = A_{22}/R_j$  are so-called crack magnitudes determined as follow

$$\gamma_{aj} = A_{11}/T_j = \gamma_{1j}\vartheta_1(R_E, n), \quad \gamma_{bj} = A_{22}/R_j = \gamma_{2j}\vartheta_2(R_E, n), \tag{29}$$

where

$$\vartheta_1(R_E, n) = (R_E + n) / (1 + n),$$

$$\vartheta_2(R_E, n) = [(3R_E + n) / 3(3 + n) - (2R_E + n) / (2 + n)\alpha + (R_E + n) / (1 + n)\alpha^2],$$

and [17, 18]

$$\gamma_{1j} = E_b b h / T_j = 2\pi(1 - \nu_0^2) h f_1(a_j / h_b), \gamma_{2j} = E_b b h^3 / R_j = 6\pi(1 - \nu_0^2) h f_2(a_j / h_b), \quad (30)$$

$$f_1(z) = z^2 \left( 0.6272 - 0.17248z + 5.92134z^2 - 10.7054z^3 + 31.5685z^4 - 67.47z^5 \right. \\ \left. + 139.123z^6 - 146.682z^7 + 92.3552z^8 \right), \quad z = a_j / h,$$

$$f_2(z) = z^2 \left( 0.6272 - 1.04533z + 4.5948z^2 - 9.9736z^3 + 20.2948z^4 - 33.0351z^5 \right. \\ \left. + 47.1063z^6 - 40.7556z^7 + 19.6z^8 \right), \quad z = a_j / h.$$

Note that the introduced crack magnitudes are dependent upon not only crack depth but also are function of the material parameters such as elasticity ratio  $R_E$  and volume fraction index  $n$ , which have been calculated only for some values of the the elasticity ratio [35].

### 2.2.3. Vibration shape

Using the traditional method in the ordinary differential equation theory, general solution of Eq. (27) for intact beam,  $\{\mathbf{Z}_0(x, \omega)\} = \{U_0(x, \omega), \Theta_0(x, \omega), W_0(x, \omega)\}^T$  can be found in the form [46]

$$\{\mathbf{Z}_0(x, \omega)\} = [\mathbf{G}_0(x, \omega)] \{\mathbf{C}\}, \quad (31)$$

where  $\{\mathbf{C}\} = (C_1, \dots, C_6)^T$  is vector of constants and  $\mathbf{G}_0(x, \omega)$  is the matrix

$$[\mathbf{G}_0(x, \omega)] = \begin{bmatrix} \alpha_1 e^{k_1 x} & \alpha_2 e^{k_2 x} & \alpha_3 e^{k_3 x} & \alpha_1 e^{-k_1 x} & \alpha_2 e^{-k_2 x} & \alpha_3 e^{-k_3 x} \\ e^{k_1 x} & e^{k_2 x} & e^{k_3 x} & e^{-k_1 x} & e^{-k_2 x} & e^{-k_3 x} \\ \beta_1 e^{k_1 x} & \beta_2 e^{k_2 x} & \beta_3 e^{k_3 x} & -\beta_1 e^{-k_1 x} & -\beta_2 e^{-k_2 x} & -\beta_3 e^{-k_3 x} \end{bmatrix}, \quad (32)$$

with  $k_1, k_2, k_3$  being the wave numbers determined from the so-called characteristic equation

$$\det[\lambda^2 \mathbf{A}_2 + \lambda \mathbf{A}_1 + \mathbf{A}_0] = 0,$$

and

$$\alpha_j = [\omega^2 I_{11} + k_j^2 A_{11}] / \omega^2 I_{12}; \beta_j = (\omega^2 I_{11} + k_j^2 A_{11}) k_j A_{33} / \omega^2 I_{12} (\omega^2 I_{11} + k_j^2 A_{33}), \quad j = 1, 2, 3. \quad (33)$$

In case of cracked beam, solution of Eq. (27),  $\{\mathbf{Z}(x, \omega)\} = \{U(x, \omega), \Theta(x, \omega), W(x, \omega)\}^T$ , satisfying conditions (28) at crack sections is [46]

$$\{\mathbf{Z}(x, \omega)\} = [\Phi(x, \omega)] \{\mathbf{C}\}, \quad (34)$$

where

$$[\Phi(x, \omega)] = [\mathbf{G}_0(x, \omega)] + \sum_{j=1}^n [\mathbf{K}(x - e_j)] \cdot [\mathbf{M}_j], \quad (35)$$

with

$$[\mathbf{K}(x)] = \begin{cases} [\mathbf{G}_c(x)] : x > 0 \\ [\mathbf{0}] : x \leq 0 \end{cases} \quad [\mathbf{K}'(x)] = \begin{cases} [\mathbf{G}'_c(x)] : x > 0 \\ [\mathbf{0}] : x \leq 0 \end{cases}$$

$$[\mathbf{G}_c(x, \omega)] = \begin{bmatrix} \gamma_a \sum_{i=1}^3 \alpha_i \delta_{i1} \cosh k_i x & \gamma_b \sum_{i=1}^3 \alpha_i (\delta_{i2} + \delta_{i3}) \cosh k_i x & 0 \\ \gamma_a \sum_{i=1}^3 \delta_{i1} \cosh k_i x & \gamma_b \sum_{i=1}^3 (\delta_{i2} + \delta_{i3}) \cosh k_i x & 0 \\ \gamma_a \sum_{i=1}^3 \beta_i \delta_{i1} \sinh k_i x & \gamma_b \sum_{i=1}^3 \beta_i (\delta_{i2} + \delta_{i3}) \sinh k_i x & 0 \end{bmatrix}, \quad (36)$$

$$\begin{aligned} \delta_{11} &= (k_3 \beta_3 - k_2 \beta_2) / \Delta, & \delta_{12} &= (\alpha_3 k_2 \beta_2 - \alpha_2 k_3 \beta_3) / \Delta, & \delta_{13} &= (\alpha_2 - \alpha_3) / \Delta, \\ \delta_{21} &= (k_1 \beta_1 - k_3 \beta_3) / \Delta, & \delta_{22} &= (\alpha_1 k_3 \beta_3 - \alpha_3 k_1 \beta_1) / \Delta, & \delta_{23} &= (\alpha_3 - \alpha_1) / \Delta, \\ \delta_{31} &= (k_2 \beta_2 - k_1 \beta_1) / \Delta, & \delta_{32} &= (\alpha_2 k_1 \beta_1 - \alpha_1 k_2 \beta_2) / \Delta, & \delta_{33} &= (\alpha_1 - \alpha_2) / \Delta, \\ \Delta &= k_1 \beta_1 (\alpha_2 - \alpha_3) + k_2 \beta_2 (\alpha_3 - \alpha_1) + k_3 \beta_3 (\alpha_1 - \alpha_2). \end{aligned}$$

Matrices  $[\mathbf{M}_j]$  are determined by recurrent relationship

$$[\mathbf{M}_j] = [\mathbf{G}'_0(e_j, \omega)] + \sum_{k=1}^{j-1} [\mathbf{G}'_c(e_j - e_k)] \cdot [\mathbf{M}_k]. \quad (37)$$

### 2.3. Functionally graded Timoshenko beam with a piezoelectric layer

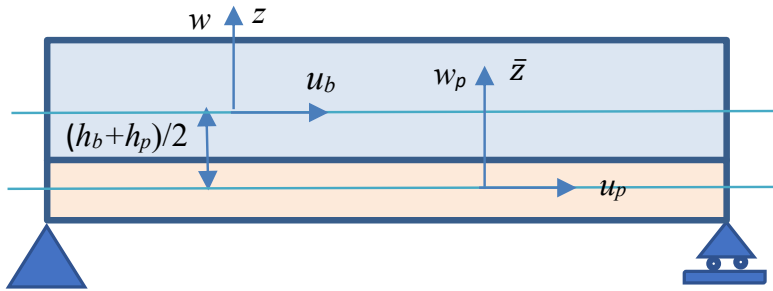


Fig. 3. Model of beam with piezoelectric layer

Let us consider a functionally graded beam of length  $L$ , width  $b$  and thickness  $h_b$  bonded with a piezoelectric layer of thickness  $h_p$  as shown in Fig. 3. Governing equations for the host beam have been given in Eqs. (23)–(24) and that equations for piezoelectric layer are represented as

$$\begin{aligned} u_p(x, \bar{z}, t) &= u_{p0}(x, t) - \bar{z} \theta_p(x, t), \quad w_p(x, \bar{z}, t) = w_{p0}(x, t); \quad \varepsilon_{px} = u'_{p0} - \bar{z} \theta'_p, \quad \gamma_p = w'_{p0} - \theta_p, \\ \sigma_{px} &= C_{11}^p \varepsilon_{px} - h_{13} D; \quad \tau_p = C_{55}^p \gamma_p; \quad \varepsilon = -h_{13} \varepsilon_{px} + \beta_{33}^p D, \end{aligned} \quad (38)$$

where  $C_{11}^p, C_{55}^p$  are elastic and shear modulus,  $h_{13}, \beta_{33}^p$  are piezoelectric and dielectric constants;  $\epsilon$  and  $D$  are electric field and displacement of the piezoelectric material.

Assume that the host beam and piezoelectric layer are perfectly bonded, and they have the same cross-section rotation so that it should be satisfied the conditions

$$u\left(x, -\frac{h_b}{2}, t\right) = u_p\left(x, \frac{h_p}{2}, t\right), \quad w\left(x, -h_b/2, t\right) = w_p\left(x, h_p/2, t\right), \quad \theta = \theta_p, \quad (39)$$

that yield

$$u_{p0} = u_0 + \theta h, \quad h = (h_b + h_p) / 2, \quad w_{p0} = w_0, \quad \epsilon_{px} = u'_0 - (\bar{z} - h) \theta', \quad \gamma_p = w'_0 - \theta.$$

Therefore, strain and kinetic energies of the integrated beam can be calculated as

$$\Pi = \Pi_b + \Pi_p = (1/2) \int_0^L \left\{ \begin{aligned} &A_{11}^* u_0'^2 + 2A_{12}^* u_0' \theta' + A_{22}^* \theta'^2 + A_{33}^* (w_0' - \theta)^2 \\ &- 2h_{13} A_p D (u_0' + h \theta') + \beta_{33}^p A_p D^2 \end{aligned} \right\} dx, \quad (40)$$

$$T = T_p + T_p = (1/2) \int_0^L \{ I_{11}^* \dot{u}_0^2 + 2I_{12}^* \dot{u}_0 \dot{\theta} + I_{22}^* \dot{\theta}^2 + I_{11}^* \dot{w}_0^2 \} dx,$$

where comma and dot denote derivative with respect to  $x$  and  $t$  respectively and

$$A_{11}^* = A_{11} + C_{11}^p A_p, \quad A_{12}^* = C_{11}^p A_p h, \quad A_{22}^* = A_{22} + C_{11}^p (I_p + A_p h^2), \quad A_{33}^* = A_{33} + C_{55}^p A_p, \\ A_p = b h_p, \quad I_{11}^* = I_{11} + \rho_p A_p, \quad I_{12}^* = \rho_p A_p h, \quad I_{22}^* = I_{22} + \rho_p I_p + \rho_p A_p h^2, \quad A_b = b h_b, \quad I_p = b h_p^3 / 12.$$

Substituting expressions (40) of total energies into Hamilton principle

$$\int_{t_1}^{t_2} \delta (T - \Pi) dt = 0,$$

allows one to obtain the equations of motion

$$\begin{aligned} &(I_{11}^* \ddot{u}_0 - B_{11}^* u_0'') + (I_{12}^* \ddot{\theta} - B_{12}^* \theta'') = 0, \\ &(I_{12}^* \ddot{u}_0 - B_{12}^* u_0'') + (I_{22}^* \ddot{\theta} - B_{22}^* \theta'') - A_{33}^* (w_0' - \theta) = 0, \\ &I_{11}^* \ddot{w}_0 - A_{33}^* (w_0'' - \theta') = 0, \end{aligned} \quad (41)$$

where

$$B_{11}^* = A_{11}^* - A_p h_{13}^2 / \beta_{33}^p = E A_b + E_p A_p, \quad B_{12}^* = A_{12}^* - A_p h h_{13}^2 / \beta_{33}^p = E_p A_p h,$$

$$B_{22}^* = A_{22}^* - A_p h^2 h_{13}^2 \beta_{33}^p = E I_b + C_{11}^p I_p + E_p A_p h^2, \quad E_p = C_{11}^p - h_{13}^2 / \beta_{33}^p,$$

and

$$D = h_{13} (u_0' + h \theta') / \beta_{33}^p. \quad (42)$$

Transferring the equations (41) into frequency domain one gets equations at the same form as Eq. (27)

$$[D_2] \{Z''\} + [D_1] \{Z'\} + [D_0] \{Z\} = 0, \quad (43)$$

but with other coefficient matrices

$$\begin{aligned}
 [\mathbf{D}_2] &= \begin{bmatrix} B_{11}^* & B_{12}^* & 0 \\ B_{12}^* & B_{22}^* & 0 \\ 0 & 0 & A_{33}^* \end{bmatrix}, \quad [\mathbf{D}_1] = \begin{bmatrix} 0 & 0 & 0 \\ 0 & 0 & A_{33}^* \\ 0 & -A_{33}^* & 0 \end{bmatrix}, \\
 [\mathbf{D}_0] &= \begin{bmatrix} \omega^2 I_{11}^* & \omega^2 I_{12}^* & 0 \\ \omega^2 I_{12}^* & \omega^2 I_{22}^* - A_{33}^* & 0 \\ 0 & 0 & \omega^2 I_{11}^* \end{bmatrix}.
 \end{aligned}$$

Eqs. (41) show that presence of the piezoelectric layer in even homogeneous beams leads also to coupling of axial and flexural vibration modes. The coupling represented by coefficients  $B_{12}^* = E_p A_p h$  and  $I_{12}^* = \rho_p A_p h$  would be both vanished if the piezoelectric layer thickness equals to zero.

So, general solution of Eq. (43) for vibration shape of cracked Timoshenko beams bonded with a piezoelectric layer,

$$\{\mathbf{Z}(x, \omega)\} = \{U(x, \omega), \Theta(x, \omega), W(x, \omega)\}^T$$

has the same form as given in Eqs. (34)–(37) with the wave numbers  $k_1, k_2, k_3$  determined from the other characteristic equation

$$\det[\lambda^2 \mathbf{D}_2 + \lambda \mathbf{D}_1 + \mathbf{D}_0] = 0. \quad (44)$$

Therefore, modal electric characteristics of the piezoelectric layer can be calculated from the solution as

$$D(x, \omega) = h_{13} [U'(x, \omega) + h\Theta'(x, \omega)] / \beta_{33}^p. \quad (45)$$

### 3. APPLICATION FOR ANALYSIS

#### 3.1. Application for modal analysis

The vibration shapes obtained above for various beam types are employed herein to develop the exact methods for dynamic analysis of cracked beam-like structures including the framed ones.

##### 3.1.1. The Transfer Matrix Method

Let us consider a framed structure consisting of multiple cracked beam elements joined each with other through connecting nodes  $x_k, k = 1, 2, \dots, n$ . Suppose that vibration shapes of the beam elements are given as

$$\{\mathbf{Z}_k(x, \omega)\} = \{U_k(x, \omega), \Theta_k(x, \omega), W_k(x, \omega)\}^T = [\Phi_k(x, \omega)] \{\mathbf{C}_k\}, k = 0, 1, 2, \dots, n + 1 \quad (46)$$

with  $\{\mathbf{C}\}$  being six-dimensional constant vector and  $[\Phi_k(x, \omega)] - 3 \times 6$  – function matrix. Introducing the so-called state vector for the  $k$ -th beam element

$$\{\mathbf{S}_k(x, \omega)\} = \{U_k(x, \omega), \Theta_k(x, \omega), W_k(x, \omega), N_k(x, \omega), M_k(x, \omega), Q_k(x, \omega)\}^T, \quad (47)$$

where  $\{\mathbf{P}_k(x, \omega)\} = \{N_k(x, \omega), M_k(x, \omega), Q_k(x, \omega)\}^T$  is internal force vector determined from the vibration shape  $\{\mathbf{Z}_k(x, \omega)\}$  as

$$\{\mathbf{P}_k(x, \omega)\} = \Re \{\mathbf{Z}_k(x, \omega)\} = [\Phi_k^N(x, \omega)] \{\mathbf{C}_k\}, \quad (48)$$

one obtains the state vector expressed in the form

$$\{\mathbf{S}_k(x, \omega)\} = [\Psi_k(x, \omega)] \{\mathbf{C}_k\}. \quad (49)$$

Substituting expression (49) into continuity conditions at the nodes  $\{\mathbf{S}_k(x_k, \omega)\} = [\Gamma_k] \{\mathbf{S}_{k-1}(x_k, \omega)\}$  with the given node transferring matrices  $[\Gamma_k]$  yields the recurrent connection

$$\{\mathbf{C}_k\} = [\bar{\Gamma}_k] \{\mathbf{C}_{k-1}\}, \quad [\bar{\Gamma}_k] = [\Psi_k(x_k, \omega)]^{-1} [\Gamma_k] [\Psi_{k-1}(x_k, \omega)],$$

that allows one to get the relationship

$$\{\mathbf{C}_k\} = [\mathbf{T}_k] \{\mathbf{C}_0\}, \quad [\mathbf{T}_k] = [\bar{\Gamma}_k \dots \bar{\Gamma}_1], \quad (50)$$

and

$$\{\mathbf{C}_{n+1}\} = [\mathbf{T}_n] \{\mathbf{C}_0\}.$$

Thus, we obtain

$$\{\mathbf{Z}_k(x, \omega)\} = [\bar{\Phi}_k(x, \omega)] \{\mathbf{C}_0\}, \quad [\bar{\Phi}_k(x, \omega)] = [\Phi_k(x, \omega) \mathbf{T}_k], \quad (51)$$

for every beam  $k$ -the segment  $k = 1, 2, \dots, n + 1$  and

$$\{\mathbf{Z}_0(x, \omega)\} = [\Phi_0(x, \omega)] \{\mathbf{C}_0\}, \quad \{\mathbf{Z}_{n+1}(x, \omega)\} = [\bar{\Phi}_{n+1}(x, \omega)] \{\mathbf{C}_0\}.$$

Applying boundary conditions for the latter expression

$$\begin{aligned} \mathcal{B}_0 \{[\Phi_0(x, \omega)]\}_{x=0} \{\mathbf{C}_0\} &= [\mathbf{B}_0] \{\mathbf{C}_0\} = 0, \\ \mathcal{B}_{n+1} \{[\bar{\Phi}_{n+1}(x, \omega)]\}_{x=\downarrow_{n+1}} \{\mathbf{C}_0\} &= [\mathbf{B}_{n+1}] \{\mathbf{C}_0\} = 0, \end{aligned}$$

or

$$[\mathbf{B}(\omega)] \{\mathbf{C}_0\} = 0, \quad [\mathbf{B}] = [\mathbf{B}_0, \mathbf{B}_{n+1}]^T. \quad (52)$$

The finally obtained equation is essential for the free vibration problem that yields the frequency equation

$$\det [\mathbf{B}(\omega)] = 0, \quad (53)$$

for finding the natural frequencies  $\omega_j, j = 1, 2, \dots$  and corresponding mode shapes

$$\{\phi_j(x)\} = [\bar{\Phi}_k(x, \omega_j)] \{\bar{\mathbf{C}}_j\}, \quad x_{k-1} < x < x_k, k = 1, \dots, n + 1, j = 1, 2, 3, \dots, \quad (54)$$

where  $\{\bar{\mathbf{C}}_j\}$  is the normalized solution of equation  $[\mathbf{B}(\omega_j)] \{\mathbf{C}\} = 0$ . These equations will be employed for modal analysis of single span, multispan and continuous beams with cracks in subsequent sections.

3.1.2. The Dynamic Stiffness Method

The developed above transfer matrix method showed to be more efficient for modal analysis of beam-like structures such as multi-span and continuous beams and it faces a difficulty in an application for framed structures. For the analysis of typical cracked framed structures, the so-called dynamic stiffness method is more appropriate because it is an enhancement of the powerful finite element method well-known in engineering applications. This subsection is devoted to developing a dynamic stiffness model of cracked frames using the vibration shapes established above for beam elements.

Thus, for a two-nodes beam element as shown in Fig. 4, where the following nodal displacement and force vectors have been introduced

$$\{\mathbf{U}_e(\omega)\} = \{U_1, \Theta_1, W_1, U_2, \Theta_2, W_2\}^T, \quad \{\mathbf{P}_e(\omega)\} = \{N_1, M_1, Q_1, N_2, M_2, Q_2\}^T, \quad (55)$$

with

$$U_1 = U(0, \omega), \Theta_1 = \Theta(0, \omega), W_1 = W(0, \omega), U_2 = U(L, \omega), \Theta_2 = \Theta(L, \omega), W_2 = W(L, \omega),$$

$$N_1 = -\mathbb{N}\{Z(x, \omega)\}_{x=0}, \quad M_1 = -\mathbb{R}\{Z(x, \omega)\}_{x=0}, \quad Q_1 = -\mathbb{Q}\{Z(x, \omega)\}_{x=0},$$

$$N_2 = \mathbb{N}\{Z(x, \omega)\}_{x=L}, \quad M_2 = \mathbb{R}\{Z(x, \omega)\}_{x=L}, \quad Q_2 = \mathbb{Q}\{Z(x, \omega)\}_{x=L},$$

or

$$\{U_1, \Theta_1, W_1\}^T = \{Z(0, \omega)\}, \quad \{U_2, \Theta_2, W_2\}^T = \{Z(L, \omega)\},$$

$$\{N_1, M_1, Q_1\}^T = \mathfrak{R}\{Z(x, \omega)\}_{x=0}, \quad \{N_2, M_2, Q_2\}^T = \mathfrak{R}\{Z(x, \omega)\}_{x=L}, \quad (56)$$

where  $\mathfrak{R} = \{\mathbb{N}, \mathbb{R}, \mathbb{Q}\}^T$  is differential vector operator with elements being operators for calculating international forces such as axial, bending moment and shear forces.

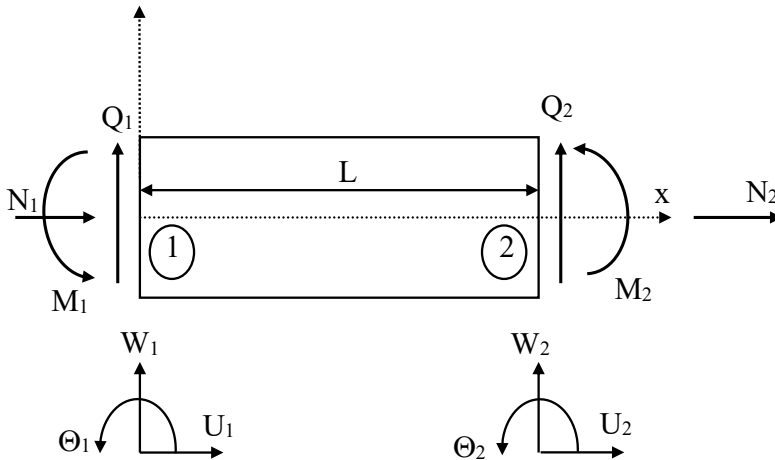


Fig. 4. Dynamic stiffness model of a beam element

Substituting expression for vibration shape  $\{\mathbf{Z}(x, \omega)\} = [\Phi(x, \omega)]\{\mathbf{C}\}$  into (56) yields

$$\begin{aligned} \{U_1, \Theta_1, W_1\}^T &= [\Phi(0, \omega)]\{\mathbf{C}\}, & \{U_2, \Theta_2, W_2\}^T &= [\Phi(L, \omega)]\{\mathbf{C}\}, \\ \{N_1, M_1, Q_1\}^T &= [\Re\Phi(x, \omega)]_{x=0}\{\mathbf{C}\}, & \{N_2, M_2, Q_2\}^T &= [\Re\Phi(x, \omega)]_{x=L}\{\mathbf{C}\}, \end{aligned} \quad (57)$$

or

$$\{\mathbf{U}_e\} = \begin{bmatrix} \Phi(0, \omega) \\ \Phi(L, \omega) \end{bmatrix} \{\mathbf{C}\}, \quad \{\mathbf{Q}_e\} = \begin{bmatrix} \Re\Phi(x, \omega)_{x=0} \\ \Re\Phi(x, \omega)_{x=L} \end{bmatrix} \{\mathbf{C}\}. \quad (58)$$

Eliminating vector  $\mathbf{C}$  from Eqs. (58) leads to

$$\{\mathbf{Q}_e\} = [\mathbf{D}_e(\omega)]\{\mathbf{U}_e\}, \quad (59)$$

where

$$[\mathbf{D}_e(\omega)] = \begin{bmatrix} \Re\Phi(x, \omega)_{x=0} \\ \Re\Phi(x, \omega)_{x=L} \end{bmatrix} \cdot \begin{bmatrix} \Phi(0, \omega) \\ \Phi(L, \omega) \end{bmatrix}^{-1}, \quad (60)$$

is called hereby dynamic stiffness matrix for the beam element.

In general case, when a given structure consists of a number of beam elements, the total dynamic stiffness matrix for the structure is assembled as accomplished in the finite element method. Namely, the dynamic stiffness matrix is

$$[\mathbf{D}(\omega)] = \sum_{e=1}^{ne} [\mathbf{T}_e]^{-1} [\mathbf{D}_e(\omega)] \cdot [\mathbf{T}_e], \quad (61)$$

where  $[\mathbf{T}_e]$  is the matrix of co-ordinate transform for  $e$ -th element.

### 3.2. Application for frequency response analysis

Now we consider equation

$$[\mathbf{D}_2] \{\mathbf{Z}''\} + [\mathbf{D}_1] \{\mathbf{Z}'\} + [\mathbf{D}_0] \{\mathbf{Z}\} = \{\mathbf{P}(x, \omega)\}, \quad (62)$$

where

$$\{\mathbf{P}(x, \omega)\} = \int_{-\infty}^{+\infty} \{\mathbf{p}(x, t)\} e^{-i\omega t} dt,$$

is Fourier Transform of the given distributed load  $\{\mathbf{p}(x, t)\}$ . Assume, furthermore, that general solution of homogeneous equation

$$[\mathbf{D}_2] \{\mathbf{Z}''\} + [\mathbf{D}_1] \{\mathbf{Z}'\} + [\mathbf{D}_0] \{\mathbf{Z}\} = 0,$$

has been found in the form

$$\{\mathbf{Z}_0(x, \omega)\} = [\Phi(x, \omega)]\{\mathbf{C}\}.$$

So, general solution of Eq. (62) can be constructed as

$$\{\mathbf{Z}(x, \omega)\} = [\Phi(x, \omega)]\{\mathbf{C}\} + \{\mathbf{Q}(x, \omega)\}, \quad (63)$$

where  $\{\mathbf{Q}(x, \omega)\}$  is a particular solution of inhomogeneous equation (62), for example,

$$\{\mathbf{Q}(x, \omega)\} = \int_0^x [\mathbf{H}(x - \tau, \omega)] \{\mathbf{P}(x, \omega)\} d\tau, \quad (64)$$

with matrix  $[\mathbf{H}(x, \omega)]$  is solution of equation

$$[\mathbf{D}_2] [\mathbf{H}'''] + [\mathbf{D}_1] [\mathbf{H}'] + [\mathbf{D}_0] [\mathbf{H}] = 0, [\mathbf{H}(0, \omega)] = [\mathbf{0}], [\mathbf{H}'(0, \omega)] = [\mathbf{D}_2]^{-1}.$$

Applying boundary conditions

$$\mathcal{B}_0 \{ \mathbf{Z}(x, \omega) \}_{x=0} = 0, \quad \mathcal{B}_L \{ \mathbf{Z}(x, \omega) \}_{x=L} = 0,$$

for solution (63) one gets

$$[\mathbf{B}_0] \{ \mathbf{C} \} = \{ \mathbf{Q}_0(\omega) \}, \quad [\mathbf{B}_L] \{ \mathbf{C} \} = \{ \mathbf{Q}_L(\omega) \}, \quad (65)$$

$$\begin{aligned} [\mathbf{B}_0(\omega)] &= \mathcal{B}_0 \{ [\Phi(x, \omega)] \}_{x=0}, & [\mathbf{B}_L(\omega)] &= \mathcal{B}_L \{ [\Phi(x, \omega)] \}_{x=L}, \\ \{ \mathbf{Q}_0(\omega) \} &= \mathcal{B}_0 \{ [\mathbf{Q}(x, \omega)] \}_{x=0}, & \{ \mathbf{Q}_L(\omega) \} &= \mathcal{B}_L \{ [\mathbf{Q}(x, \omega)] \}_{x=L}. \end{aligned} \quad (66)$$

Consequently, we can find vector as

$$\{ \mathbf{C} \} = - \begin{bmatrix} \mathbf{B}_0(\omega) \\ \mathbf{B}_L(\omega) \end{bmatrix}^{-1} \begin{Bmatrix} \mathbf{Q}_0(\omega) \\ \mathbf{Q}_L(\omega) \end{Bmatrix},$$

and solution (63) satisfying the boundary conditions would be

$$\{ \mathbf{Z}(x, \omega) \} = \{ \mathbf{Q}(x, \omega) \} - [\Phi(x, \omega)] \begin{bmatrix} \mathbf{B}_0(\omega) \\ \mathbf{B}_L(\omega) \end{bmatrix}^{-1} \begin{Bmatrix} \mathbf{Q}_0(\omega) \\ \mathbf{Q}_L(\omega) \end{Bmatrix}. \quad (67)$$

This is frequency response of the beam to external load  $\{ \mathbf{p}(x, t) \}$ . For instance, in case of point impulse

$$\{ \mathbf{p}(x, t) \} = P_0 \{ 0, 0, 1 \}^T \delta(x - x_0) \delta(t),$$

one has

$$\{ \mathbf{Q}(x, \omega) \} = P_0 \{ \mathbf{H}_3(x - x_0) \},$$

where

$$\mathbf{H}_3(x) = \{ 0, \text{ for } x < x_0 \text{ or } \mathbf{h}_3(x) \text{ for } x \geq x_0 \},$$

and  $\mathbf{h}_3(x)$  is the third column of the matrix  $[\mathbf{H}(x, \omega)]$ .

## 4. NUMERICAL EXAMPLES

### 4.1. Modal analysis of cracked functionally graded beams

#### 4.1.1. Single span functionally graded beams

First, modal analysis of single span FGM beam with single crack is conducted using Eq. (53) that can be rewritten in the form

$$\det [\mathbf{B}(\omega, e, a, r, n)] = 0, \quad (68)$$

where  $e, a$  are crack location and depth,  $r = E_t/E_b$  is the top-to-bottom elasticity modulus ratio,  $n$  – the volume fraction index and matrix  $\mathbf{B}(\omega, e, a, r, n) = [\mathbf{B}_0(\omega, e, a, r, n), \mathbf{B}_L(\omega, e, a, r, n)]^T$  with

$$\begin{aligned} [\mathbf{B}_0(\omega, a, e, r, n)] &= \mathcal{B}_0 \{ [\Phi(x, \omega, e, a, r, n)] \}_{x=0}, \\ [\mathbf{B}_L(\omega, a, e, r, n)] &= \mathcal{B}_L \{ [\Phi(x, \omega, e, a, r, n)] \}_{x=L}. \end{aligned} \quad (69)$$

Thus, natural frequencies of the beams can be found by solving Eq. (68) with respect to  $\omega$  in dependence upon crack location  $e$  and depth  $a$ , elasticity modulus ratio  $r$  and

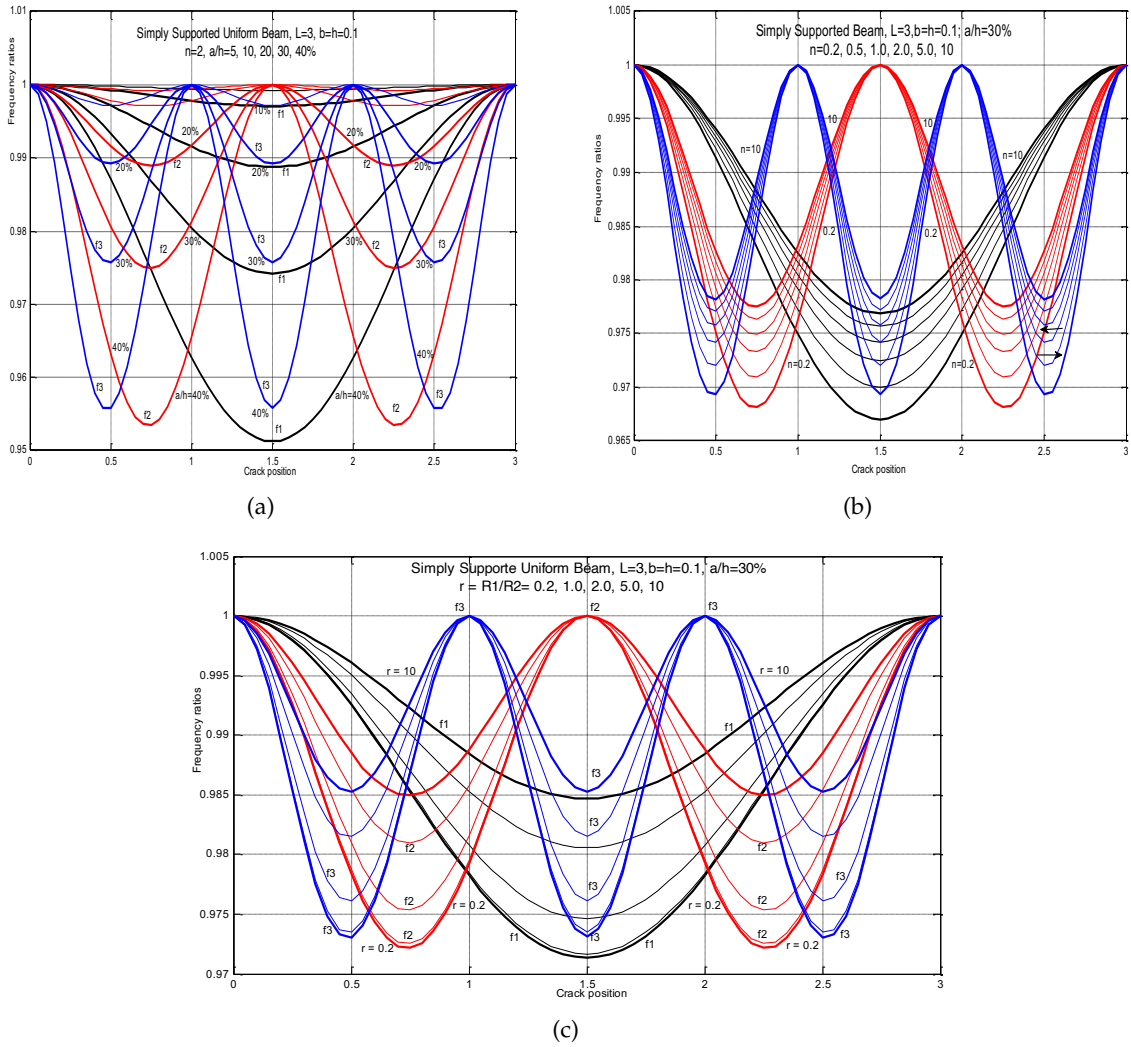


Fig. 5. Normalized three lowest natural frequencies of simply supported FGM beam in dependence on the crack depth (a), fraction index  $n$  (b) and elasticity modulus ratio  $r$  (c)

volume fraction index  $n$ . Obviously, natural frequencies obtained for  $a = 0$  are natural frequencies of undamaged beams and in case if  $n = 0$  roots of the equation provide natural frequencies of homogeneous beams. Therefore, crack-induced change in natural frequencies of FGM beam represented by the natural frequencies of cracked beams normalized by those of undamaged ones can be computed as function of crack location  $e$  in different (a) crack depth, (b) elasticity modulus ratio and (c) fraction index  $n$ . The normalized natural frequencies are computed for beams in conventional cases of boundary conditions such as simple supports (SS), clamped ends (CC) and cantilever (CF) and results of computation are presented in Figs. 5–7 respectively for the boundary conditions

cases. It can be seen from the Figures that the natural frequency variation for FGM beams versus crack location and depth is similar to that for homogeneous beams and the variation increases with decreasing both top-to-bottom elasticity modulus ratio and volume fraction index ( $n$ ). Also, there exist positions on FGM beams occurred at which crack makes no effect on a particular natural frequency. Such locations are called frequency nodes and the nodes are independent of material grading indexes.

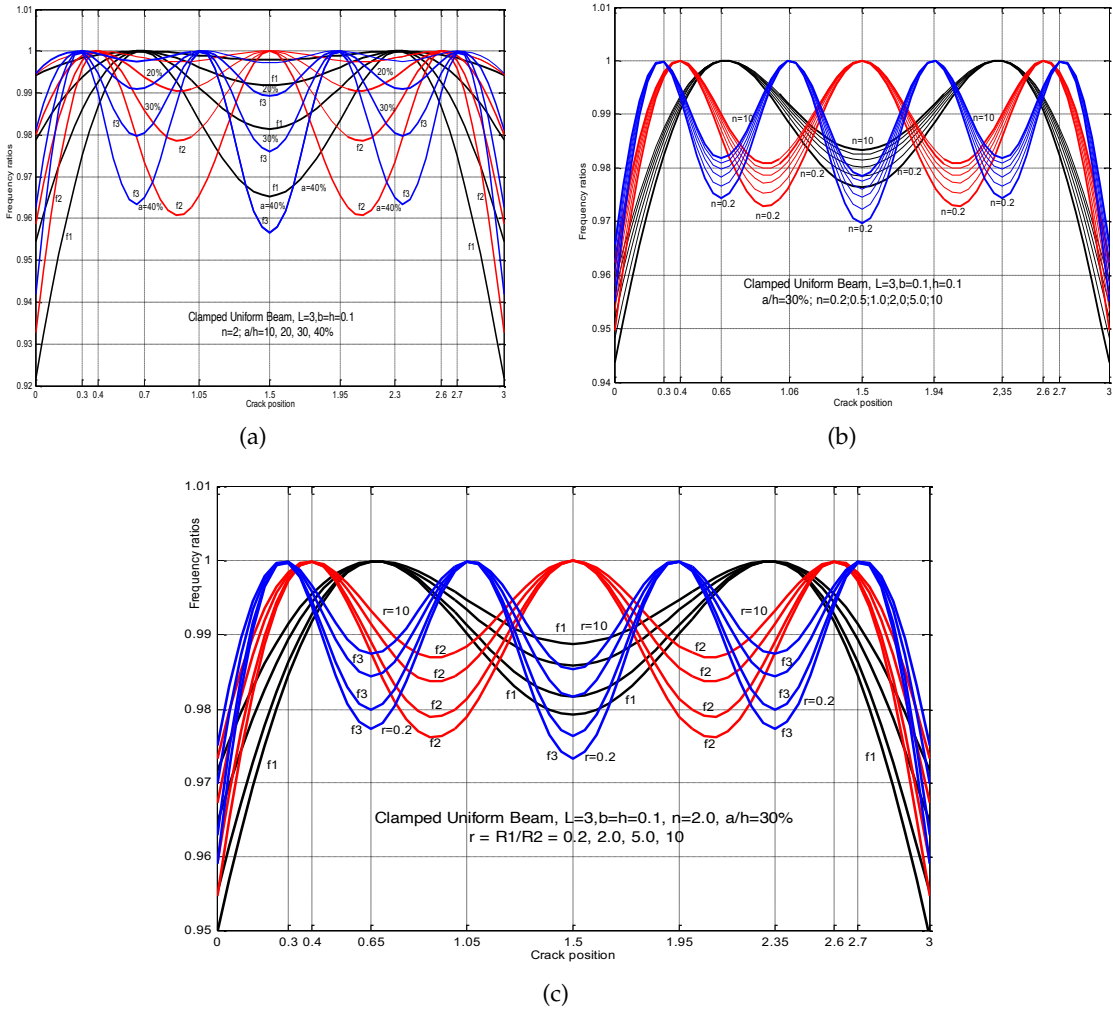


Fig. 6. Normalized three lowest natural frequencies of uniform clamped FGM beam in dependence on the crack depth (a), fraction index  $n$  (b) and elasticity modulus ratio (c)

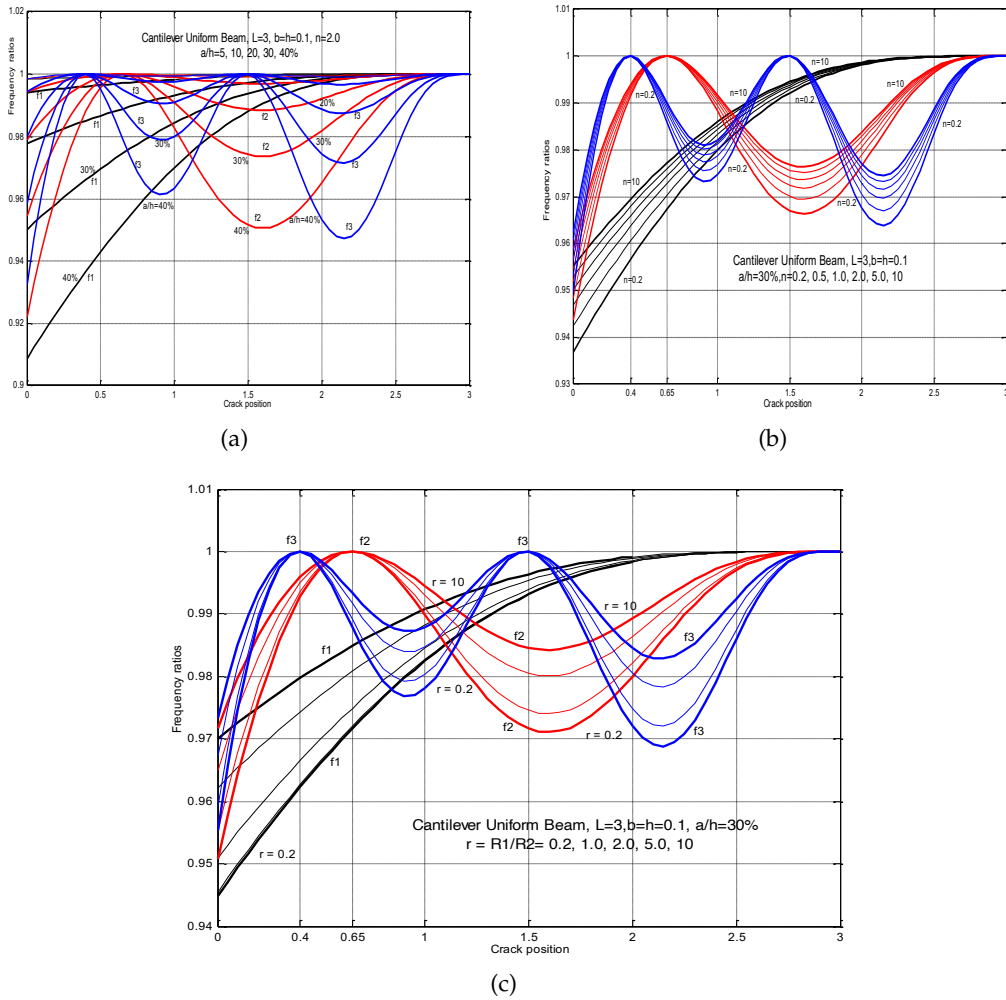


Fig. 7. Normalized three lowest natural frequencies of uniform cantilever FGM beam in dependence on the crack depth (a), fraction index  $n$  (b) and elasticity modulus ratio (c)

4.1.2. Continuous functionally graded beams

Next, for illustrating the Transfer Matrix Method developed for modal analysis of cracked FGM structures, we consider herein also the change in natural frequencies of cracked continuous FGM beam.

Namely, the equation (53) is solved for cracked FGM beam with two rigid supports (three spans) in dependence on the crack and material parameters. Normalized first frequency of bending (Figs. 8–9) and longitudinal (Fig. 10) vibrations in the simply supported (a) and clamped (b) continuous beam is examined as function of crack location running along three spans for various crack depth and material grading index. It is observed that the change in natural frequencies of multi-span FGM beams versus crack

depth and material grading index  $n$  is similar to that of single span beam. Moreover, the positions of the intermediate supports are nodes of fundamental frequency in flexural vibration for simply supported multi-span beams and the effect of crack on natural frequencies of axial vibration modes is independent of the presence of the intermediate supports.

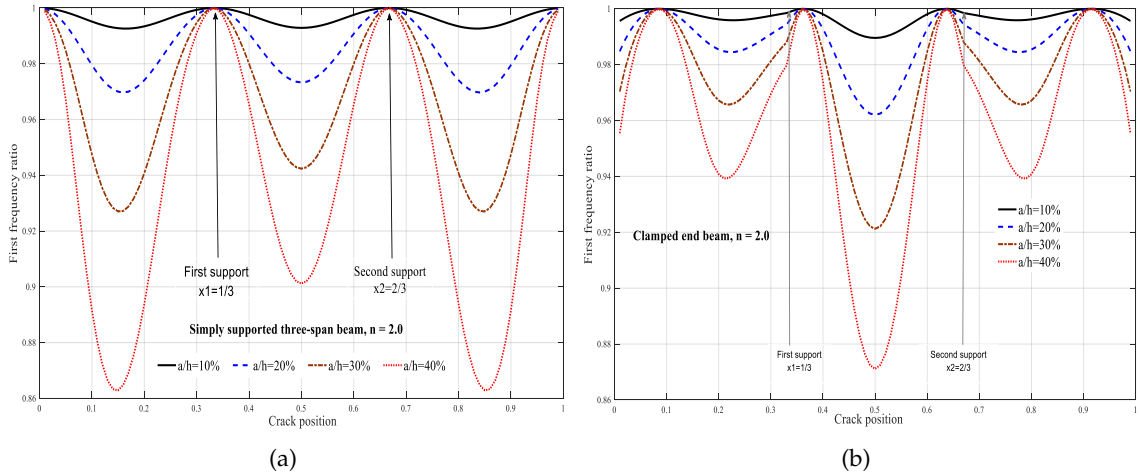


Fig. 8. Normalized first flexural frequency of three-span FGM beam (a – SSB, b – CCB) as function of crack location in various relative crack depth ( $a/h$ )

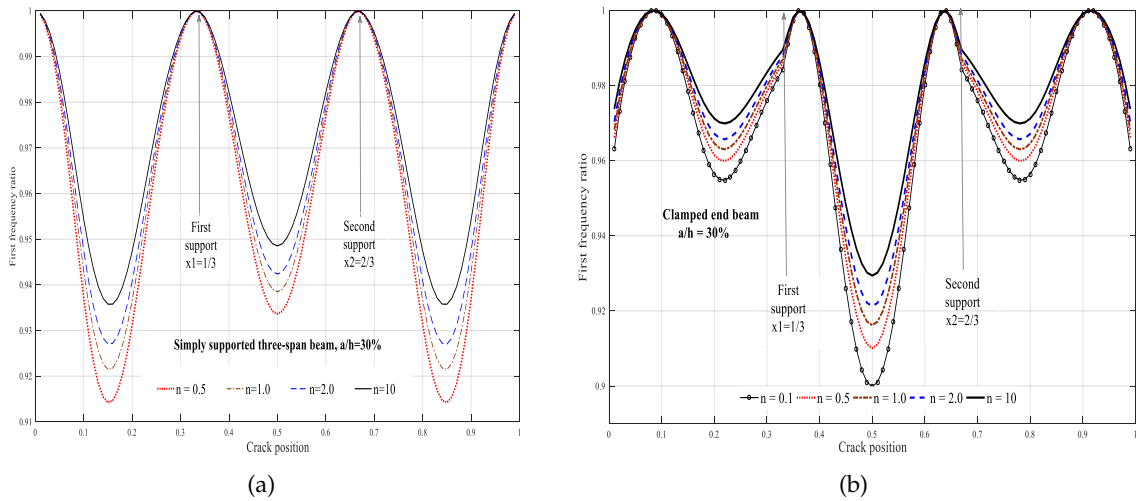


Fig. 9. Normalized first flexural frequency of three-span FGM beam (a – SSB, b – CCB) as function of crack location in various material grading index ( $n$ )

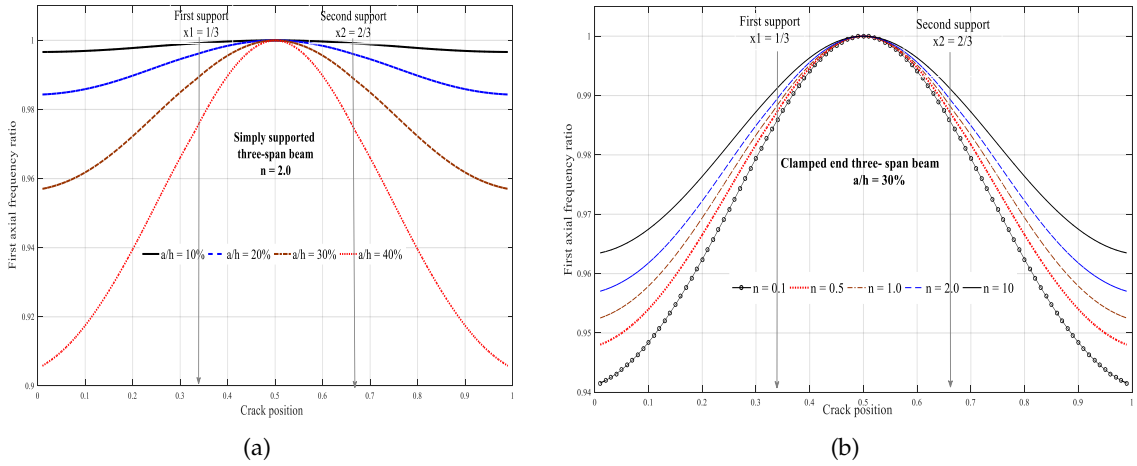


Fig. 10. Normalized first axial frequency of three-span FGM beam (a – SSB, b – CCB) as function of crack location in various crack depth (a) and material grading index (b)

4.1.3. Stepped functionally graded beams

Finally, the proposed dynamic stiffness method is applied for modal analysis of cracked functionally graded beams with three steps that are shown in Fig. 11.

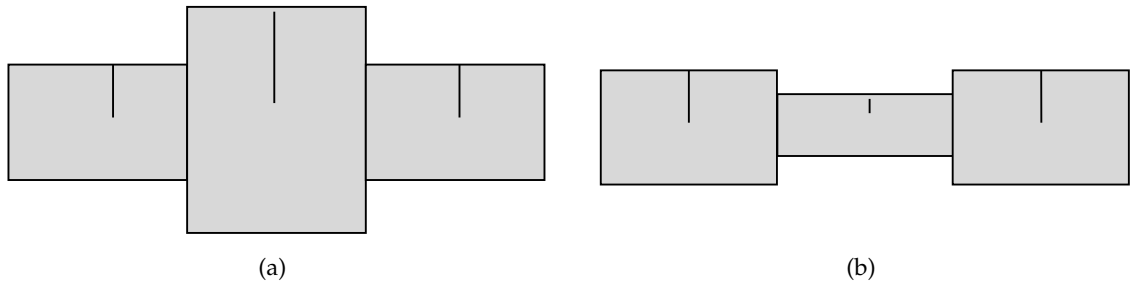


Fig. 11. Model of stepped functionally graded beam: (a) step-up beam; (b) step-down beam

Normalized natural frequencies of lowest modes for stepped beams shown in Figs. 12–17 as functions of crack location in different crack depth (Figs. 12–14), volume fraction index (Fig. 15–17) demonstrate that increase of cross-section area leads to decrease of natural frequency sensitivity to crack.

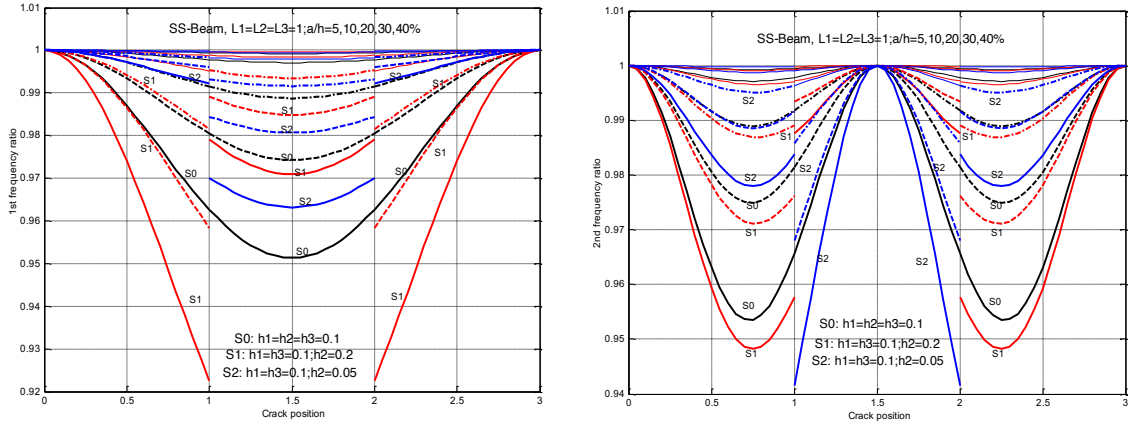


Fig. 12. Variation of two lowest natural frequencies versus crack location in various crack depth for simply supported beam (SSB)

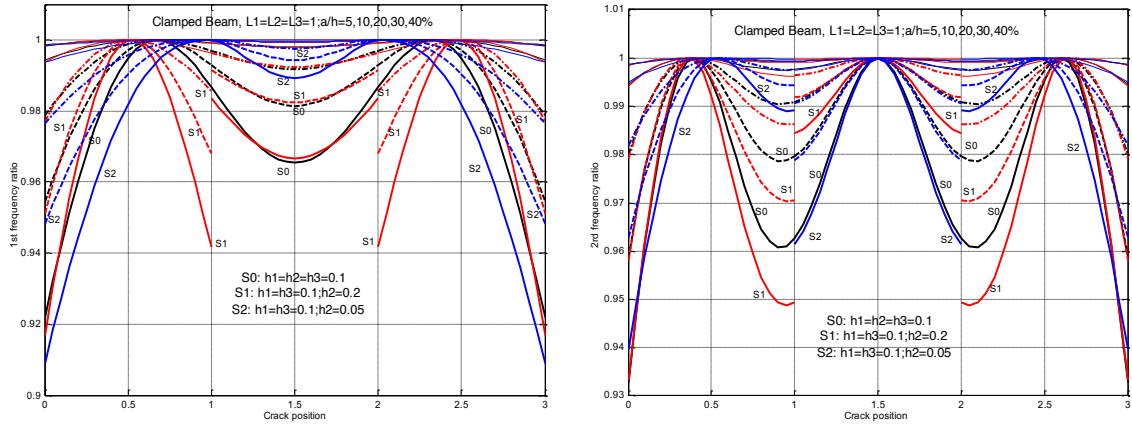


Fig. 13. Variation of two lowest natural frequencies versus crack location in various crack depth for clamped end beam (CEB)

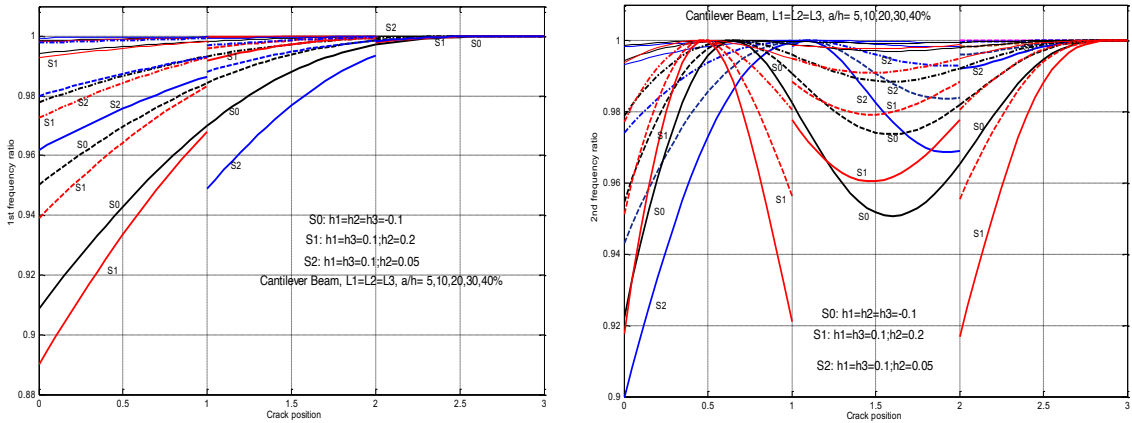


Fig. 14. Variation of two lowest natural frequencies versus crack location in various crack depth for cantilever beam (CFB)

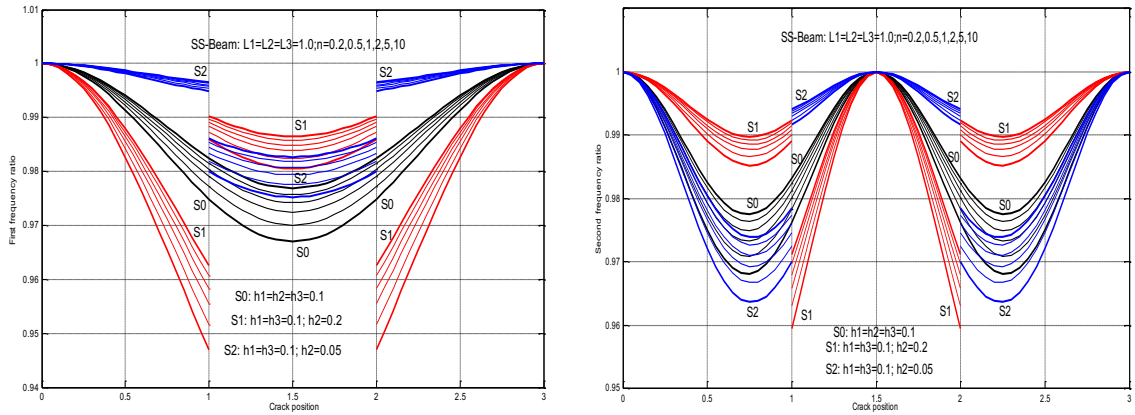


Fig. 15. Variation of two lowest natural frequencies versus crack location in various fraction index for simply supported beam (SS)

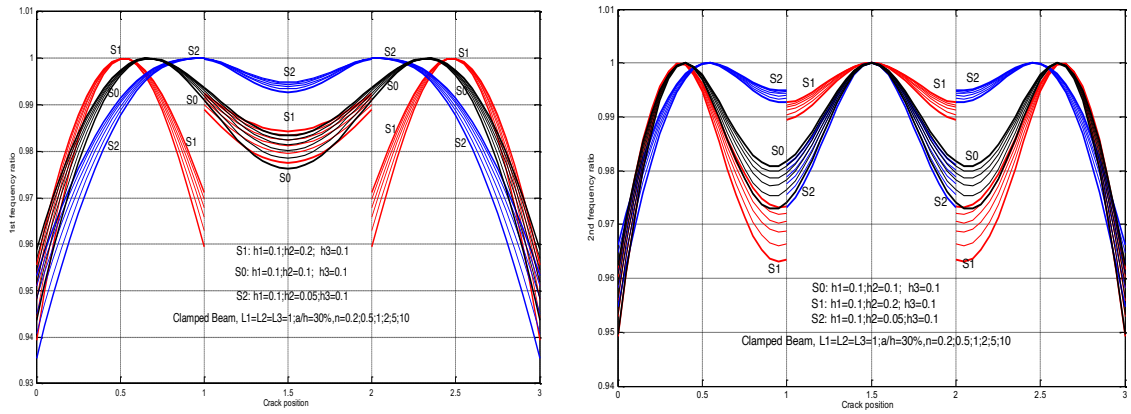


Fig. 16. Variation of two lowest natural frequencies versus crack location in various fraction index for clamped end beam (CC)

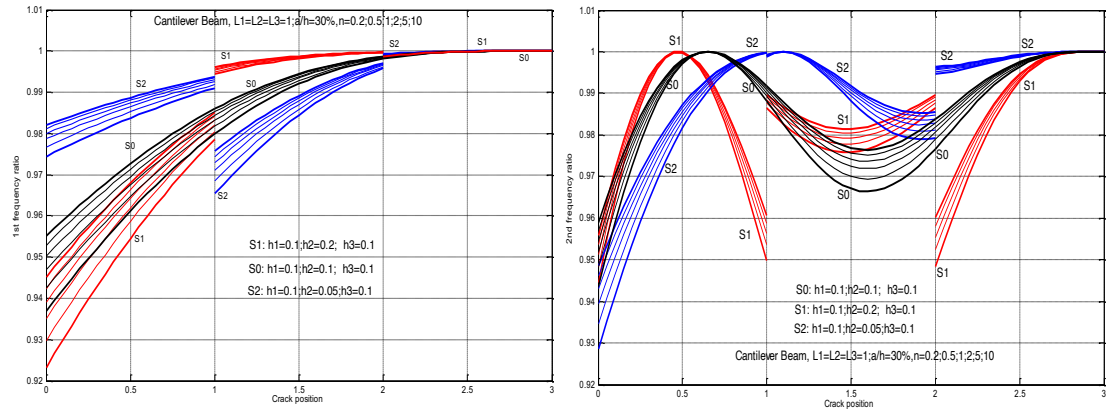


Fig. 17. Variation of two lowest natural frequencies versus crack location in various fraction index for Cantilever beam (CF)

**4.2. Free and forced vibration of cracked Timoshenko beams with piezoelectric layer**

**4.2.1. Modal analysis cracked FGM beams with piezoelectric layer**

Let's consider free vibration of simply supported FGM beam with a piezoelectric layer described by Eq. (43) general solution of which is given as

$$\{Z(x, \omega)\} = \{U(x, \omega), \Theta(x, \omega), W(x, \omega)\}^T = [\Phi(x, \omega)] \{C\}, \tag{70}$$

Putting expression (70) into boundary conditions

$$U(0) = W(0) = M(0) = U(L) = W(L) = M(L) = 0,$$

with  $M(x) = B_{12}^* \partial_x U(x) - B_{22}^* \partial_x \Theta(x)$ , one gets

$$[B(\omega)] \{C\} = 0, \tag{71}$$

where

$$[B(\omega)] = [B_{SS}(\omega)] = \begin{bmatrix} \alpha_1 & \alpha_2 & \alpha_3 & \alpha_1 & \alpha_2 & \alpha_3 \\ \beta_1 & \beta_2 & \beta_3 & -\beta_1 & -\beta_2 & -\beta_3 \\ m_1 & m_2 & m_3 & -m_1 & -m_2 & -m_3 \\ \phi_{11}(L) & \phi_{12}(L) & \phi_{13}(L) & \phi_{14}(L) & \phi_{15}(L) & \phi_{16}(L) \\ \phi_{31}(L) & \phi_{32}(L) & \phi_{33}(L) & \phi_{34}(L) & \phi_{35}(L) & \phi_{36}(L) \\ M_1(L) & M_2(L) & M_3(L) & M_4(L) & M_5(L) & M_6(L) \end{bmatrix},$$

$$m_j = (B_{12}^* \alpha_j - B_{22}^*) k_j, j = 1, 2, 3; M_j(L) = B_{12}^* \phi'_{1j}(L) - B_{22}^* \phi'_{2j}(L), j = 1, 2, \dots, 6,$$

$\phi_{ij}(x), \phi'_{ij}(x), i = 1, 2, 3; j = 1, 2, \dots, 6$  are elements of matrices  $[\Phi(x, \omega)]$  and  $[\Phi'(x, \omega)]$  defined in (35). Therefore, so-called frequency equation of the beam is obtained in the form

$$\det [B(\omega)] = 0, \tag{72}$$

that allows one to find natural frequencies  $\omega_1, \omega_2, \omega_3, \dots$  of the piezoelectric beam. For every given natural frequency  $\omega_k$ , a normalized of solution of Eq. (71) can be easily found as  $(\vartheta_1, \dots, \vartheta_6)$  that allow calculating corresponding mode shape as

$$U_k(x) = C_k \left( \alpha_1 \vartheta_1 e^{k_1 x} + \alpha_2 \vartheta_2 e^{k_2 x} + \alpha_3 \vartheta_3 e^{k_3 x} + \alpha_1 \vartheta_4 e^{-k_1 x} + \alpha_2 \vartheta_5 e^{-k_2 x} + \alpha_3 \vartheta_6 e^{-k_3 x} \right),$$

$$\Theta_k(x) = C_k \left( \vartheta_1 e^{k_1 x} + \vartheta_2 e^{k_2 x} + \vartheta_3 e^{k_3 x} + \vartheta_4 e^{-k_1 x} + \vartheta_5 e^{-k_2 x} + \vartheta_6 e^{-k_3 x} \right), \tag{73}$$

$$W_k(x) = C_k \left( \beta_1 \vartheta_1 e^{k_1 x} + \beta_2 \vartheta_2 e^{k_2 x} + \beta_3 \vartheta_3 e^{k_3 x} - \beta_1 \vartheta_4 e^{-k_1 x} - \beta_2 \vartheta_5 e^{-k_2 x} - \beta_3 \vartheta_6 e^{-k_3 x} \right),$$

where arbitrary constant  $C_k$  can be obtained from a chosen mode shape normalization, for instance,

$$\max_x |W_k(x)| = 1.$$

Using the mode shape, it can be calculated so-called hereby modal sensor output (MSO) charge generated in the piezoelectric layer as

$$Q_k = (bh_{13}/\beta_{33}^p) \int_0^L [U'_k(x) - h\Theta'_k(x)/2] dx$$

$$= (bh_{13}/\beta_{33}^p) \{ [U_k(L) - U_k(0) - \gamma_1 U'_k(e)] - (h/2) [\Theta_k(L) - \Theta_k(0) - \gamma_2 \Theta'_k(e)] \}, \tag{74}$$

where  $\gamma_1, \gamma_2$  are magnitudes of single cracks at position  $e$  defined above in Eq. (30). This modal sensor output will be numerically examined below mutually with natural frequencies and mode shapes of FGM beam with piezoelectric layer with the following input data for the beam

$$L_b = L_p = L = 1 \text{ m}, b = 0.1 \text{ m}, h_b = L/10,$$

$$E_t = 390 \text{ MPa}, \rho_t = 3960 \text{ kg/m}^3, \mu_t = 0.25; E_b = 210 \text{ MPa}, \rho_b = 7800 \text{ kg/m}^3, \mu_t = 0.31,$$

$$C_{11}^p = 69.0084 \text{ GPa}, C_{55}^p = 21.0526 \text{ GPa}, \rho_p = 7750 \text{ kg/m}^3, h_{13} = -7.70394 \times 10^8 \text{ V/m}$$

Since the influence of piezoelectric layer on sensitivity of modal parameters such as natural frequencies and mode shapes of functionally graded beam to crack is insignificant, herein we focus on the effect of crack and material grading index on modal sensor output of the piezoelectric layer calculated by expression (74). Namely, the sensor charge of first and third modes versus crack location in various crack depth, material grading

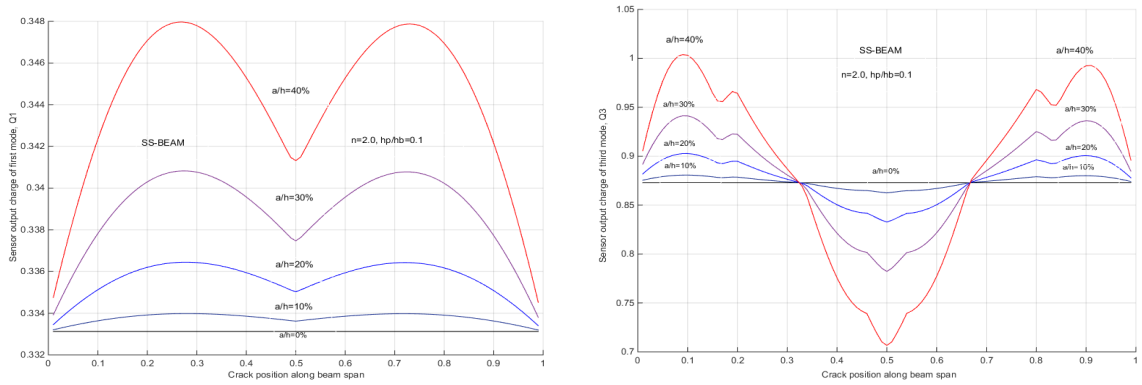


Fig. 18. Crack-induced variation of modal sensor output charge in various crack depth

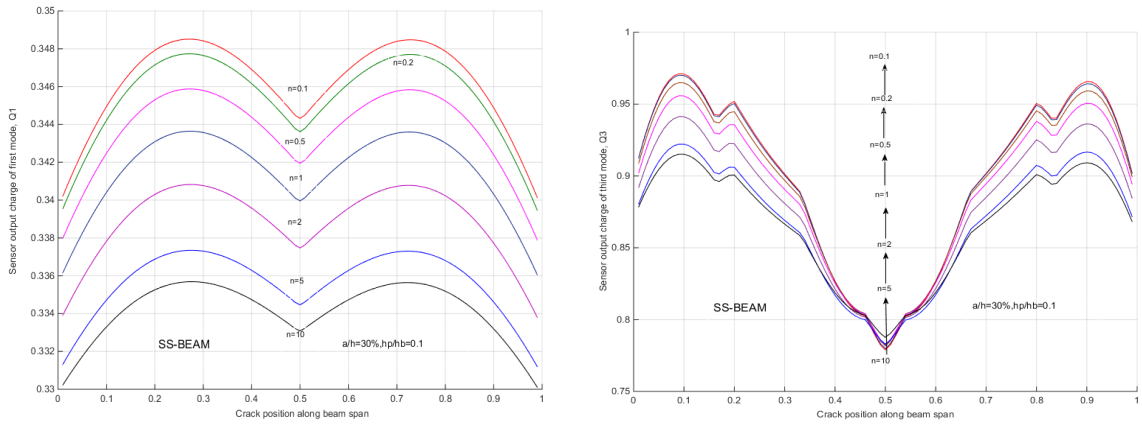


Fig. 19. Crack-induced variation of modal sensor outputs charge in various material gradient index  $n$

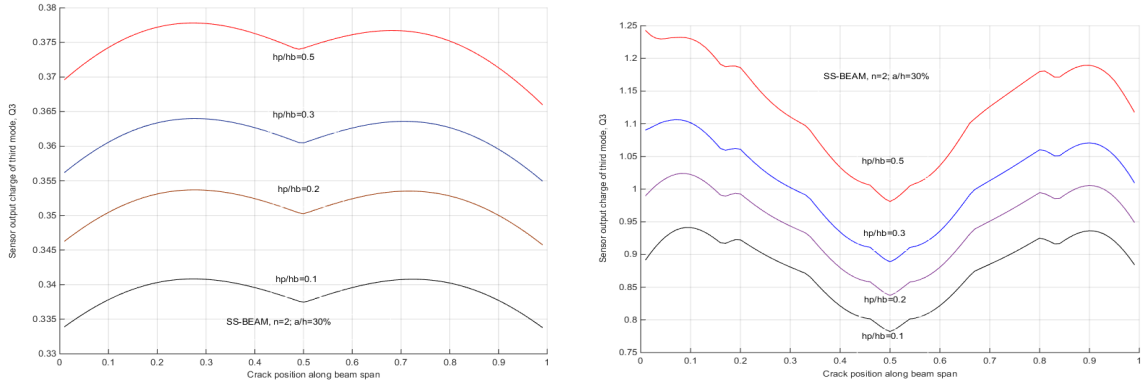


Fig. 20. Crack-induced variation of modal sensor outputs charge in various thickness of piezoelectric layer

index and piezoelectric layer thickness have been computed and results of computation are given in Figs. 18–20. The charge computed for the second mode is very miniature so that is not provided in the Figures. Graphs depicted in the Figures show that an increase in crack depth and thickness of the piezoelectric layer-sensor leads to an increase in the modal sensor charges, while the growth of the material grading index reduces the charges. It is interesting to note that the sensor output charge of the third mode has two nodes where an occurred crack has no effect on it.

#### 4.2.2. Frequency response of cracked FGM beam with piezoelectric layer to moving load

The frequency response of cracked FGM beam with a piezoelectric layer obtained in previous section, the expression (67), is numerically examined herein for harmonic load moving on the beam with constant speed  $p(x, t) = P_0 e^{i\Omega_m t} \delta(x - vt)$ . In this case

$$\{\mathbf{P}(x, \omega)\} = \int_{-\infty}^{+\infty} \{0, 0, p(x, t)\}^T e^{-i\omega t} dt = \{0, 0, P_0/v\}^T e^{i(\Omega_m - \omega)x/v}, \quad (75)$$

that allows one to find a particular solution of Eq. (62) in the form

$$\{\mathbf{Q}(x, \omega)\} = \{U_q^0(\omega), \Theta_q^0(\omega), W_q^0(\omega)\}^T \exp\{i\Omega x/v\}, \quad \Omega = (\Omega_m - \omega), \quad (76)$$

where

$$U_q^0(\omega) = (i\Omega) Q_0 A_{33}^* (\Omega^2 B_{12}^* - \omega^2 I_{12}^*) / \Delta, \quad \Theta_q^0(\omega) = (i\Omega) Q_0 A_{33}^* (\omega^2 I_{11}^* - \Omega^2 B_{11}^*) / \Delta, \\ W_q^0(\omega) = Q_0 D / \Delta, \quad \Delta = (\omega^2 I_{11}^* - \Omega^2 A_{33}^*) D + i\Omega A_{33}^{*2} (\omega^2 I_{11}^* - \Omega^2 B_{11}^*), \quad (77)$$

$$D = \omega^4 (I_{11}^* I_{22}^* - I_{12}^{*2}) + \Omega^4 (B_{11}^* B_{22}^* - B_{12}^{*2}) + A_{33}^* (\Omega^2 B_{11}^* - \omega^2 I_{11}^*) \\ + \omega^2 \Omega^2 (2I_{12}^* B_{12}^* - I_{11}^* B_{22}^* - I_{22}^* B_{11}^*).$$

Therefore, solution (67) for simply supported beam gets the form

$$\{\mathbf{Z}_m(x, \omega)\} = \{\mathbf{Q}(x, \omega)\} - [\Phi(x, \omega)] [\mathbf{B}(\omega)]^{-1} \{\hat{\mathbf{P}}(\omega)\}, \quad (78)$$

with matrix  $[B(\omega)]$  given by Eq. (71) and

$$\begin{aligned} \hat{P}_1(\omega) &= U_q^0(\omega), \quad \hat{P}_2(\omega) = \Theta_q^0(\omega), \quad \hat{P}_3(\omega) = W_q^0(\omega), \\ \hat{P}_4(\omega) &= U_q^0(\omega) \exp\{-i\Omega L\}, \quad \hat{P}_5(\omega) = \Theta_q^0(\omega) \exp\{-i\Omega L\}, \\ \hat{P}_6(\omega) &= W_q^0(\omega) \exp\{-i\Omega L\}. \end{aligned} \tag{79}$$

In case of beam with single crack, frequency-dependent sensor output charge, acknowledged herein as electrical frequency response of piezoelectric layer-sensor, can be calculated as

$$\begin{aligned} Q_p(\omega) &= (bh_{13}/\beta_{33}^p) \int_0^L [U'_m(x, \omega) + h\Theta'_m(x, \omega)] dx \\ &= (bh_{13}/\beta_{33}^p) \{ [U_m(L, \omega) - U_m(0, \omega) - \gamma_1 U'_m(e, \omega)] \\ &\quad + h [\Theta_m(L, \omega) - \Theta_m(0, \omega) - \gamma_2 \Theta'_m(e, \omega)] \}, \end{aligned} \tag{80}$$

with crack magnitudes  $\gamma_1, \gamma_2$  defined above in Eq. (30).

Analysis of the electrical frequency response (80) conducted in [50] for various parameters of the moving load shows that under a certain speed of the moving load it can be clearly observed the vibration component of eigenfrequency (eigenmode vibration component) mutually with the steady forced vibration component. Moreover, amplitude of the eigenmode vibration component is more sensitive to crack than that of the forced one, especially, when the load frequency closes to the eigenfrequency of intact beam ( $\Omega_m = \omega_{01}$ ). Such vibration component is acknowledged as generic resonant vibration, amplitude of which is examined below in dependence upon crack, load and material parameters. Namely, graphs given in Figs. 21–23 are generic resonant amplitudes

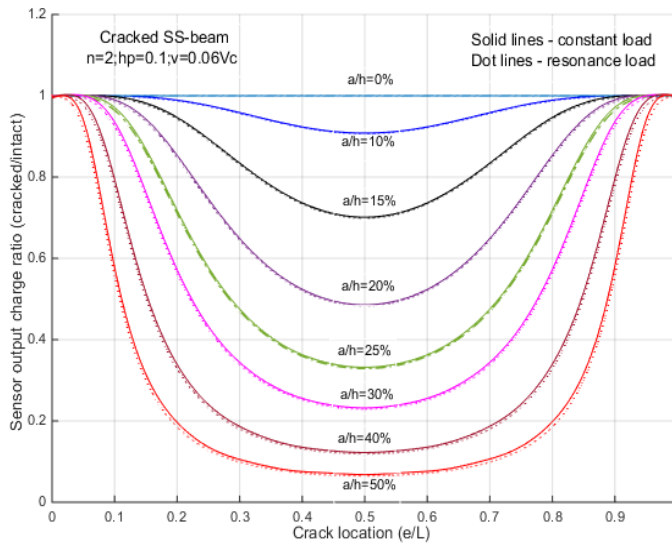


Fig. 21. Crack-induced variation (cracked/intact) of first eigenmodes amplitude of sensor output charge at generic resonant harmonic force

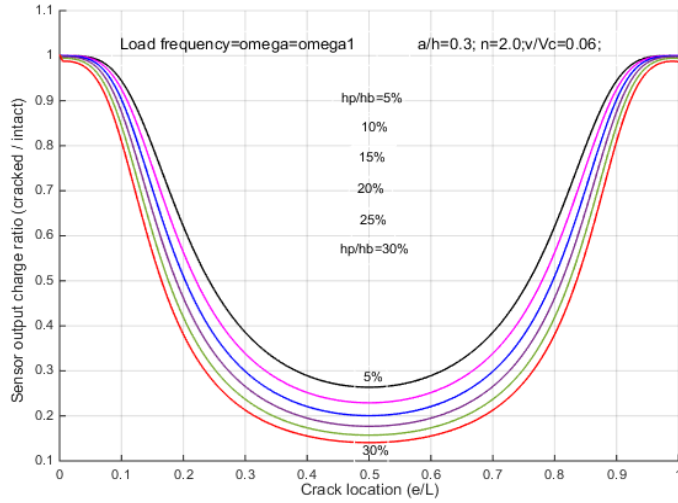


Fig. 22. Effect of piezoelectric layer thickness ( $h_p$ ) on crack-induced change in eigenmode amplitude of sensor output charge at generic resonant harmonic force

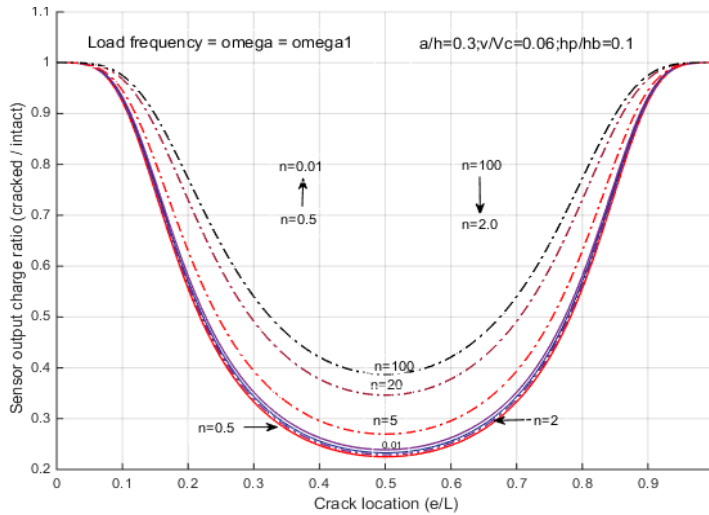


Fig. 23. Effect of material grading index ( $n$ ) on crack-induced change in eigenmode amplitude of sensor output charge at generic resonant harmonic force

of cracked SS-beam normalized by those of uncracked one as function of crack location for various crack depth, material grading index and piezoelectric layer thickness respectively. For comparison, there are presented in the Figures also the normalized amplitudes computed for constant load ( $\Omega_m = 0$ ) represented by the solid lines.

Observing the graphs demonstrated in the Figures enables us to make the following remarks: First, crack-induced variation of the eigenmode resonant vibration amplitude

versus crack location is similar to that of fundamental frequency, but it is much more sensitive to crack depth than the natural frequency; Second, an increase in the piezoelectric layer thickness leads to the growth of the crack-induced change in the vibration amplitude. Finally, the crack-induced change reaches its maximum when  $n = 0.5$  and load frequency makes no effect on the sensitivity of the vibration amplitude to crack. This provides important indications for crack detection by measurement of the response of the beam to the moving load.

## 5. CONCLUSIONS

Thus, this review article presented a unified approach to vibration analysis of cracked beam structures that is based on general solution of the equations of motion in the frequency domain called herein as frequency-dependent vibration shape functions. The shape functions were obtained in an explicit expression for uniform beam elements with multiple cracks modeled by the equivalent springs so that enable one to use the minimum number of beam elements for vibration analysis of multiple cracked frame structures. Moreover, the vibration shape functions have been constructed not only for homogeneous beams but also for functionally graded beams so that allow vibration analysis of cracked structures made of functionally graded materials. Numerical illustrations show usefulness of the proposed approach to study both free and forced vibrations of multi-span, multistep cracked FGM beams with different boundary conditions.

## DECLARATION OF COMPETING INTEREST

The authors declare that they have no known competing financial interests or personal relationships that could have appeared to influence the work reported in this paper.

## FUNDING

This research received no specific grant from any funding agency in the public, commercial, or not-for-profit sectors.

## REFERENCES

- [1] J. K. Kottke and R. H. Menning. *Detection of a transverse crack in a turbine shaft - the Oak Creek experience*. A.S.M.E., Paper 81-JPGC-Pwr-19, (1981).
- [2] N. Anifantis, N. Aspragathos, and A. D. Dimarogonas. Diagnosis of cracks on concrete frames due to earthquakes by vibration response analysis. In *3rd International Symposium of International Measurements Federation (IMEKO)*, Moscow, (1983).
- [3] P. F. Rizos, N. Aspragathos, and A. D. Dimarogonas. Identification of crack location and magnitude in a cantilever beam from the vibration modes. *Journal of Sound and Vibration*, **138**, (1990), pp. 381–388. [https://doi.org/10.1016/0022-460x\(90\)90593-o](https://doi.org/10.1016/0022-460x(90)90593-o).
- [4] O. S. Salawu. Detection of structural damage through changes in frequency: a review. *Engineering Structures*, **19**, (1997), pp. 718–723. [https://doi.org/10.1016/s0141-0296\(96\)00149-6](https://doi.org/10.1016/s0141-0296(96)00149-6).
- [5] N. Papaeconomou and A. Dimarogonas. Vibration of cracked beams. *Computational Mechanics*, **5**, (2-3), (1989), pp. 88–94. <https://doi.org/10.1007/bf01046477>.
- [6] A. D. Dimarogonas. Vibration of cracked structures: A state of the art review. *Engineering Fracture Mechanics*, **55**, (1996), pp. 831–857. [https://doi.org/10.1016/0013-7944\(94\)00175-8](https://doi.org/10.1016/0013-7944(94)00175-8).

- [7] P. Gudmundson. Eigenfrequency changes of structures due to cracks, notches or other geometrical changes. *Journal of the Mechanics and Physics of Solids*, **30**, (1982), pp. 339–353. [https://doi.org/10.1016/0022-5096\(82\)90004-7](https://doi.org/10.1016/0022-5096(82)90004-7).
- [8] S. Christides and A. D. S. Barr. One-dimensional theory of cracked Bernoulli-Euler beams. *International Journal of Mechanical Sciences*, **26**, (1984), pp. 639–648. [https://doi.org/10.1016/0020-7403\(84\)90017-1](https://doi.org/10.1016/0020-7403(84)90017-1).
- [9] M.-H. H. Shen and C. Pierre. Natural modes of Bernoulli-Euler beams with symmetric cracks. *Journal of Sound and Vibration*, **138**, (1990), pp. 115–134. [https://doi.org/10.1016/0022-460x\(90\)90707-7](https://doi.org/10.1016/0022-460x(90)90707-7).
- [10] M.-H. H. Shen and C. Pierre. Free vibrations of beams with a single-edge crack. *Journal of Sound and Vibration*, **170**, (1994), pp. 237–259. <https://doi.org/10.1006/jsvi.1994.1058>.
- [11] G. R. Irwin. Analysis of stresses and strains near the end of a crack traversing a plate. *Journal of Applied Mechanics*, **24**, (1957), pp. 361–364. <https://doi.org/10.1115/1.4011547>.
- [12] R. A. Westmann and W. H. Yang. Stress analysis of cracked rectangular beams. *Journal of Applied Mechanics*, **34**, (1967), pp. 693–701. <https://doi.org/10.1115/1.3607763>.
- [13] A. D. Dimarogonas and Paipetis. *Analytical methods in rotor dynamics*. London: Elsevier Applied Science, (1983).
- [14] G. Gounaris and A. Dimarogonas. A finite element of a cracked prismatic beam for structural analysis. *Computers & Structures*, **28**, (1988), pp. 309–313. [https://doi.org/10.1016/0045-7949\(88\)90070-3](https://doi.org/10.1016/0045-7949(88)90070-3).
- [15] R. D. Adams, P. Cawley, C. J. Pye, and B. J. Stone. A vibration technique for non-destructively assessing the integrity of structures. *Journal of Mechanical Engineering Science*, **20**, (1978), pp. 93–100. <https://doi.org/10.1243/jmes.jour.1978.020.016.02>.
- [16] W. M. Ostachowicz and M. Krawczuk. Analysis of the effect of cracks on the natural frequencies of a cantilever beam. *Journal of Sound and Vibration*, **150**, (1991), pp. 191–201. [https://doi.org/10.1016/0022-460x\(91\)90615-q](https://doi.org/10.1016/0022-460x(91)90615-q).
- [17] T. G. Chondros, A. D. Dimarogonas, and J. Yao. A continuous cracked beam theory. *Journal of Sound and Vibration*, **215**, (1998), pp. 17–34. <https://doi.org/10.1006/jsvi.1998.1640>.
- [18] T. G. Chondros, A. D. Dimarogonas, and J. Yao. Longitudinal vibration of a continuous cracked bar. *Engineering Fracture Mechanics*, **61**, (1998), pp. 593–606. [https://doi.org/10.1016/s0013-7944\(98\)00071-x](https://doi.org/10.1016/s0013-7944(98)00071-x).
- [19] B. Biondi and S. Caddemi. Closed form solutions of Euler-Bernoulli beams with singularities. *International Journal of Solids and Structures*, **42**, (2005), pp. 3027–3044. <https://doi.org/10.1016/j.ijsolstr.2004.09.048>.
- [20] S. Caddemi and I. Caliò. Exact closed-form solution for the vibration modes of the Euler-Bernoulli beam with multiple open cracks. *Journal of Sound and Vibration*, **327**, (2009), pp. 473–489. <https://doi.org/10.1016/j.jsv.2009.07.008>.
- [21] A. Morassi. Crack-induced changes in eigenparameters of beam structures. *Journal of Engineering Mechanics*, **119**, (1993), pp. 1798–1803. [https://doi.org/10.1061/\(asce\)0733-9399\(1993\)119:9\(1798\)](https://doi.org/10.1061/(asce)0733-9399(1993)119:9(1798)).
- [22] Y. Narkis. Identification of crack location in vibrating simply supported beams. *Journal of Sound and Vibration*, **172**, (1994), pp. 549–558. <https://doi.org/10.1006/jsvi.1994.1195>.
- [23] E. I. Shifrin and R. Ruotolo. Natural frequencies of a beam with an arbitrary number of cracks. *Journal of Sound and Vibration*, **222**, (1999), pp. 409–423. <https://doi.org/10.1006/jsvi.1998.2083>.

- [24] N. T. Khiem and T. V. Lien. A simplified method for natural frequency analysis of multiple cracked beam. *Journal of Sound and Vibration*, **245**, (2001), pp. 737–751. <https://doi.org/10.1006/jsvi.2001.3585>.
- [25] Q. S. Li. Free vibration analysis of non-uniform beams with an arbitrary number of cracks and concentrated masses. *Journal of Sound and Vibration*, **252**, (2002), pp. 509–525. <https://doi.org/10.1006/jsvi.2001.4034>.
- [26] N. T. Khiem and T. T. Hai. A closed-form solution for free vibration of beams with arbitrary number of cracks. In *Proceedings of the Scientific Conference dedicated to 35th Anniversary of Vietnam Academy of Science and Technology*, Hanoi, Vol. 1, (2010), pp. 30–42.
- [27] S. P. Lele and S. K. Maiti. Modeling of transverse vibration of short beams for crack detection and measurement of crack extension. *Journal of Sound and Vibration*, **257**, (2002), pp. 559–583. <https://doi.org/10.1006/jsvi.2002.5059>.
- [28] M. Krawczuk, M. Palacz, and W. Ostachowicz. The dynamic analysis of a cracked Timoshenko beam by the spectral element method. *Journal of Sound and Vibration*, **264**, (2003), pp. 1139–1153. [https://doi.org/10.1016/s0022-460x\(02\)01387-1](https://doi.org/10.1016/s0022-460x(02)01387-1).
- [29] Q. S. Li. Vibratory characteristics of Timoshenko beams with arbitrary number of cracks. *Journal of Engineering Mechanics*, **129**, (2003), pp. 1355–1359. [https://doi.org/10.1061/\(asce\)0733-9399\(2003\)129:11\(1355\)](https://doi.org/10.1061/(asce)0733-9399(2003)129:11(1355)).
- [30] J. A. Loya, L. Rubio, and J. Fernández-Sáez. Natural frequencies for bending vibrations of Timoshenko cracked beams. *Journal of Sound and Vibration*, **290**, (2006), pp. 640–653. <https://doi.org/10.1016/j.jsv.2005.04.005>.
- [31] N. T. Khiem and D. T. Hung. A closed-form solution for free vibration of multiple cracked Timoshenko beam and application. *Vietnam Journal of Mechanics*, **39**, (2017), pp. 315–328. <https://doi.org/10.15625/0866-7136/9641>.
- [32] F. Erdogan and B. H. Wu. The surface crack problem for a plate with functionally graded properties. *Journal of Applied Mechanics*, **64**, (1997), pp. 449–456. <https://doi.org/10.1115/1.2788914>.
- [33] X.-F. Li. A unified approach for analyzing static and dynamic behaviors of functionally graded Timoshenko and Euler–Bernoulli beams. *Journal of Sound and Vibration*, **318**, (2008), pp. 1210–1229. <https://doi.org/10.1016/j.jsv.2008.04.056>.
- [34] J. Yang and Y. Chen. Free vibration and buckling analyses of functionally graded beams with edge cracks. *Composite Structures*, **83**, (2008), pp. 48–60. <https://doi.org/10.1016/j.compstruct.2007.03.006>.
- [35] S. Kitipornchai, L. L. Ke, J. Yang, and Y. Xiang. Nonlinear vibration of edge cracked functionally graded Timoshenko beams. *Journal of Sound and Vibration*, **324**, (2009), pp. 962–982. <https://doi.org/10.1016/j.jsv.2009.02.023>.
- [36] S. A. Sina, H. M. Navazi, and H. Haddadpour. An analytical method for free vibration analysis of functionally graded beams. *Materials & Design*, **30**, (2009), pp. 741–747. <https://doi.org/10.1016/j.matdes.2008.05.015>.
- [37] Z. Yu and F. Chu. Identification of crack in functionally graded material beams using the p-version of finite element method. *Journal of Sound and Vibration*, **325**, (2009), pp. 69–84. <https://doi.org/10.1016/j.jsv.2009.03.010>.
- [38] T. Yan, S. Kitipornchai, J. Yang, and X. Q. He. Dynamic behaviour of edge-cracked shear deformable functionally graded beams on an elastic foundation under a moving load. *Composite Structures*, **93**, (2011), pp. 2992–3001. <https://doi.org/10.1016/j.compstruct.2011.05.003>.

- [39] K. Aydin. Free vibration of functionally graded beams with arbitrary number of surface cracks. *European Journal of Mechanics - A/Solids*, **42**, (2013), pp. 112–124. <https://doi.org/10.1016/j.euromechsol.2013.05.002>.
- [40] Ş. D. Akbaş. Free vibration characteristics of edge cracked functionally graded beams by using finite element method. *International Journal of Engineering Trends and Technology*, **4**, (10), (2013), pp. 4590–4597.
- [41] M. A. Eltaher, A. E. Alshorbagy, and F. F. Mahmoud. Determination of neutral axis position and its effect on natural frequencies of functionally graded macro/nanobeams. *Composite Structures*, **99**, (2013), pp. 193–201. <https://doi.org/10.1016/j.compstruct.2012.11.039>.
- [42] H. Su and J. R. Banerjee. Development of dynamic stiffness method for free vibration of functionally graded Timoshenko beams. *Computers & Structures*, **147**, (2015), pp. 107–116. <https://doi.org/10.1016/j.compstruc.2014.10.001>.
- [43] D. Gayen, R. Tiwari, and D. Chakraborty. Static and dynamic analyses of cracked functionally graded structural components: A review. *Composites Part B: Engineering*, **173**, (2019). <https://doi.org/10.1016/j.compositesb.2019.106982>.
- [44] G. P. Sinha and B. Kumar. Review on vibration analysis of functionally graded material structural components with cracks. *Journal of Vibration Engineering & Technologies*, **9**, (2020), pp. 23–49. <https://doi.org/10.1007/s42417-020-00208-3>.
- [45] N. T. Khiem, N. N. Huyen, and N. T. Long. Vibration of cracked Timoshenko beam made of functionally graded material. In *Shock & Vibration, Aircraft/Aerospace, Energy Harvesting, Acoustics & Optics, Volume 9*. Springer International Publishing, (2017), pp. 133–143. [https://doi.org/10.1007/978-3-319-54735-0\\_15](https://doi.org/10.1007/978-3-319-54735-0_15).
- [46] T. V. Lien, N. T. Duc, and N. T. Khiem. Free vibration analysis of multiple cracked functionally graded Timoshenko beams. *Latin American Journal of Solids and Structures*, **14**, (2017), pp. 1752–1766. <https://doi.org/10.1590/1679-78253693>.
- [47] T. V. Lien, N. T. Duc, and N. T. Khiem. Free and forced vibration analysis of multiple cracked FGM multi span continuous beams using dynamic stiffness method. *Latin American Journal of Solids and Structures*, **16**, (2), (2019). <https://doi.org/10.1590/1679-78255242>.
- [48] N. T. Khiem, T. T. Hai, and L. Q. Huong. Effect of piezoelectric patch on natural frequencies of Timoshenko beam made of functionally graded material. *Materials Research Express*, **7**, (2020). <https://doi.org/10.1088/2053-1591/ab8df5>.
- [49] N. T. Khiem, T. T. Hai, and L. Q. Huong. Modal analysis of cracked FGM beam with piezoelectric layer. *Mechanics Based Design of Structures and Machines*, (2021), pp. 1–21. <https://doi.org/10.1080/15397734.2021.1992775>.
- [50] N. T. Khiem, D. T. Huan, and T. T. Hieu. Vibration of cracked FGM beam with piezoelectric layer under moving load. *Journal of Vibration Engineering & Technologies*, (2022). <https://doi.org/10.1007/s42417-022-00607-8>.